NRL Memorandum Report 5792

A Collisional-Radiative Model and Saha Decrements for a Nonequilibrium Oxygen Plasma

R. D. TAYLOR* AND A. W. ALI

Plasma Physics Division

**Berkeley Research Associates*
Springfield, VA 22150

May 20, 1986

This work was supported by the Defense Advanced Research Projects Agency under ARPA Order 4395, Amendment #54, and monitored by the Naval Surface Weapons Center under Contract #N60921-85-WR-W0239.

NAVAL RESEARCH LABORATORY
Washington, D.C.

SECURITY CLASSIFICATION OF THIS PAGE

REPORT DOCUMENTATION PAGE

1a. REPORT SECURITY CLASSIFICATION UNCLASSIFIED	1b. RESTRICTIVE MARKINGS
2a. SECURITY CLASSIFICATION AUTHORITY	3. DISTRIBUTION / AVAILABILITY OF REPORT Approved for public release; distribution unlimited.
2b. DECLASSIFICATION / DOWNGRADING SCHEDULE	
4. PERFORMING ORGANIZATION REPORT NUMBER(S) NRL Memorandum Report 5792	5. MONITORING ORGANIZATION REPORT NUMBER(S)
6a. NAME OF PERFORMING ORGANIZATION Naval Research Laboratory 6b. OFFICE SYMBOL (If applicable) Code 4700.1	7a. NAME OF MONITORING ORGANIZATION Naval Surface Weapons Center
6c. ADDRESS (City, State, and ZIP Code) Washington, DC 20375-5000	7b. ADDRESS (City, State, and ZIP Code) Silver Spring, MD 20903
8a. NAME OF FUNDING / SPONSORING ORGANIZATION DARPA 8b. OFFICE SYMBOL (If applicable)	9. PROCUREMENT INSTRUMENT IDENTIFICATION NUMBER
8c. ADDRESS (City, State, and ZIP Code) Arlington, VA 22209	10. SOURCE OF FUNDING NUMBERS PROGRAM ELEMENT NO. 62707E; PROJECT NO.; TASK NO.; WORK UNIT ACCESSION NO. DN680-415
11. TITLE (Include Security Classification) A Collisional-Radiative Model and Saha Decrements for a Nonequilibrium Oxygen Plasma	
12. PERSONAL AUTHOR(S) Taylor, R. D.* and Ali, A. W.	
13a. TYPE OF REPORT Interim 13b. TIME COVERED FROM _____ TO _____	14. DATE OF REPORT (Year, Month, Day) 1986 May 20 15. PAGE COUNT 48
16. SUPPLEMENTARY NOTATION *Berkeley Research Associates, Springfield, VA 22150 (Continues)	

17. COSATI CODES			18. SUBJECT TERMS (Continue on reverse if necessary and identify by block number)	
FIELD	GROUP	SUB-GROUP	Collisional-radiative model	Oxygen plasma
			Saha decrements	LTE and NonLTE

19. ABSTRACT (Continue on reverse if necessary and identify by block number)

Using a time dependent approach a collisional-radiative model is developed for an oxygen plasma. Effective recombination and ionization coefficients are calculated for two specific cases, optically thin and optically thick in bound-bound UV radiation. The steady state population densities for neutral and ionic states are presented in terms of their deviations from Saha equilibrium predictions. These results show the approach of the plasma to a state of local thermodynamic equilibrium (LTE) as a function of electron temperatures between 1.0 and 3.0 eV and electron densities between 10^{16} and 10^{19} cm^{-3}.

10 to the 16th power

10 to the 19th power/cc

20. DISTRIBUTION / AVAILABILITY OF ABSTRACT ☒ UNCLASSIFIED/UNLIMITED ☐ SAME AS RPT. ☐ DTIC USERS	21. ABSTRACT SECURITY CLASSIFICATION UNCLASSIFIED
22a. NAME OF RESPONSIBLE INDIVIDUAL A. W. Ali	22b. TELEPHONE (Include Area Code) (202) 767-3762 22c. OFFICE SYMBOL Code 4700.1

DD FORM 1473, 84 MAR 83 APR edition may be used until exhausted. All other editions are obsolete.

SECURITY CLASSIFICATION OF THIS PAGE

16. SUPPLEMENTARY NOTATION (Continued)

This work was supported by the Defense Advanced Research Projects Agency under ARPA Order 4395, Amendment #54, and monitored by the Naval Surface Weapons Center under Contract #N60921-85-WR-W0239.

CONTENTS

A COLLISIONAL-RADIATIVE MODEL AND SAHA DECREMENTS FOR A NONEQUILIBRIUM OXYGEN PLASMA

I. INTRODUCTION

When air is heated and becomes highly ionized, the primary constituents consist of nitrogen, oxygen and their ions. Emissions from this plasma provide diagnostic information as well as contribute to cooling the plasma. To describe such a plasma under nonequilibrium conditions one must know the population densities of various excited states. Previously, we developed[1,2] a collisional-radiative model for nitrogen and its ions to provide this information for electron temperatures Te = 1-3 eV and electron densities Ne > 1.0×10^{16} cm^{-3}. In this report we extend the model to oxygen and its ions over the same electron temperature and density regime, thereby providing the basis for a collisional-radiative model for air at these temperatures and densities.

The model was motivated by the earlier work of Bates et al.[3-6] on hydrogen and hydrogenic ions. In contrast to Bates et al. we solve the time dependent rate equations explicitly, for a fixed electron temperature, and calculate effective collisional-radiative recombination and ionization coefficients from the steady state results. The final state populations are compared to those expected if Saha equilibrium conditions are satisfied, giving a quantitative

Manuscript approved March 31, 1986.

measure of the extent to which the plasma is in LTE. A comprehensive description of the model can be found elsewhere.[1,2]

The computations in this report are for an optically thin oxygen plasma and an optically thick case where bound-bound uv radiation is totally reabsorbed.

II. COLLISIONAL-RADIATIVE MODEL

A. Energy Level Model

For electron temperatures in the range 1-3 eV the important ions are O^+ and O^{++}. We have included in our calculation the lowest 17 levels for O I, the lowest 15 levels for O II, and two representative levels for O III. Details are presented in Tables 1 through 3.

Within this model the bound-bound radiation is listed in Table 4; each transition is described by its wavelength, the number given by Wiese et al.[7], spectral character, transition index (e.g., 6+ - 1+ denotes emission from level 6 to level 1 in O^+), and transition energy. This table shows, for example, that visible emission comes from both O and O^+. Therefore, one expects this radiation to be important as soon as excited O is produced.

The threshold values (excitation energies) for free-bound radiation are listed in Table 5.

B. Collisional and Radiative Processes

The coupled rate equations which describe the evolution of the oxygen plasma include the following collisional and radiative processes: collisional excitation and de-excitation of O and O^+, collisional ionization of O and O^+, two-body and three-body recombination of O^+ and O^{++}, and spontaneous emission from O and O^+ excited states. For the optically thin plasma photo-ionization and absorption are excluded. For the optically thick case complete absorption is assumed for the uv lines, while photo-ionization and absorption of the other lines are neglected.

The rate coefficients for these processes are computed using formulas analogous to those discussed in references [1,2] for the nitrogen plasma. They represent the most recent information available and where possible are scaled to experimental data. In addition, electron impact excitation coefficients for transitions amongst the ground state configurations of O and O^+ are discussed by Ali et al.[8]

The coupled rate equations are also modified to account for the reduction in ionization potential that occurs when an electron-ion pair resides in a plasma as opposed to an isolated environment. This effect is discussed in detail by Griem[9]; our modifications are discussed in references [1,2].

C. Collisional-Radiative Coefficients

The collisional-radiative recombination and ionization coefficients account for the net effect of collisional ionization, three-body recombination, and radiative recombination in a simple way. Denoting α^o_{Cr} and α^+_{CR} as the effective recombination coefficients for O^+ -> O and O^{++} -> O^+ and S^o_{CR} and S^+_{CR} as the effective ionization coefficients for the reverse processes, the rate equations for O, O^+, O^{++}, and Ne may be written compactly as

$$\frac{dO}{dt} = Ne\ O^+\ \alpha^o_{CR} - Ne\ O\ S^o_{CR} \tag{1}$$

$$\frac{dO^+}{dt} = -\ Ne\ O^+\ \alpha^o_{CR} + Ne\ O\ S^o_{CR} + Ne\ O^{++}\ \alpha^+_{CR} - Ne\ O^+\ S^+_{CR} \tag{2}$$

$$\frac{dO^{++}}{dt} = Ne\ O^+\ S^+_{CR} - Ne\ O^{++}\ \alpha^+_{CR} \tag{3}$$

$$\frac{dNe}{dt} = Ne\ O\ S^o_{CR} + Ne\ O^+\ S^+_{CR} - Ne\ O^+\ \alpha^o_{CR} - Ne\ O^{++}\ \alpha^+_{CR} \tag{4}$$

The steady state values of the coefficients are presented in Tables 6 - 9 for the thin case and 10 - 13 for the thick case as a function of the final electron density and electron temperature. Te is kept constant throughout the integration while Ne and the rest of the species evolve in time.

The coefficients reveal the same behavior seen in the nitrogen cases. At high electron densities the recombination coefficient is linearly proportional to Ne, a consequence of the dominance of three-body recombination over two-body for Ne > 10^{18} cm^{-3}. For lower electron densities the effective coefficient approaches the two-body value. There is very little difference between the optically thin and thick recombination results. The optically thin collisional-radiative ionization coefficients show a rapid rise with Ne for low electron densities (Ne < 10^{17} cm^{-3}) and a slower rise for higher densities (Ne > 10^{18} cm^{-3}) while approaching saturation. For high electron densities the optically thin and thick ionization coefficients are comparable, in this region the plasma is collision-dominated. However, at low densities the optically thick ionization coefficients exceed the thin values by as much as an order of magnitude if the temperature is low (e.g. Ne = 10^{16} cm^{-3}, Te = 1.0 eV).

These are the first calculations of collisional-radiative coefficients for oxygen which use a time dependent approach. Contrasting these results to those of nitrogen[1,2], it is seen that at low temperatures the neutral recombination and ionization coefficients for oxygen are approximately a factor of 5 larger than those for nitrogen

for both thin and thick cases. This occurs because the slope of the ionization cross section near threshold is higher for oxygen and the ionization potential is lower by approximately 1.0 eV.[10] The ionization coefficients for O^+ are less than those of N^+ for both thin and thick cases. This results because the ionization potential for N^+ is approximately 5.5 eV less than that for O^+. The recombination coefficients for O^+ are also less than the corresponding N^+ values.

III. SAHA DECREMENTS

When collisional transition rates exceed the corresponding radiative transitions the plasma is collision-dominated. It is then possible to specify the populations of the constituent species by using the Boltzmann-Saha equation at the local electron temperature[9]. This corresponds to a state of LTE, the onset of which depends on Ne and Te. For example, it was found[1,2] that for a nitrogen plasma LTE is valid for Ne > 10^{18} cm^{-3} for Te = 1-3 eV. The Saha decrement proves to be a useful quantitative measure for the onset of LTE. In particular, the Saha decrement is defined as the ratio of the level population computed from solving the rate equations, $O^{z-1}(n)$, to the population obtained by solving the Saha equation for each stage of ionization, $O_s^{z-1}(n)$. The specific level is indicated by the index n and z-1 corresponds to the ionization stage (z=1 for neutral, z>1 for ions). The Saha decrement is given by

$$\rho^{z-1}(n) = \frac{O^{z-1}(n)}{O_s^{z-1}(n)} \qquad (5)$$

As a working criteria[9] equilibrium is achieved when the relevant Saha decrements are within 10% of unity.

The Saha decrements for an optically thin oxygen plasma for Te = 1-3 eV are presented in Figs. 1-20. The results show the following: First, for any given Te, as the number of electrons increases equilibrium is achieved for excited O I states before excited O II states and, as expected, for

the excited neutral and ionic states before the ground states. The onset of equilibrium depends only weakly on Te for oxygen. All O states are in equilibrium for $Ne > 2.0 \times 10^{18}$ cm^{-3} for the temperatures of interest. Excited O states are generally in equilibrium for $Ne > 2.0 \times 10^{17}$ cm^{-3}, or slightly larger if Te = 1.0 eV. Griem[9] and others require that the electron de-excitation rate of the resonance line must exceed ten times the radiative decay for LTE to exist. For the oxygen atom the 5 - 1 transition (see Table 4) satisfies this criteria for $Ne > 2.7 \times 10^{18}$ cm^{-3} for Te = 1.0 eV. For O^+ equilibrium is not attained until $Ne > 6.0 \times 10^{18}$ cm^{-3}; the highly excited states require $Ne > 2.0 \times 10^{18}$ cm^{-3}.

IV. CONCLUDING REMARKS

The recombination and ionization processes for an optically thin, homogeneous, charge neutral oxygen plasma have been studied for electron densities between 10^{16} cm^{-3} and 10^{19} cm^{-3} and electron temperatures from 1.0 eV to 3.0 eV. Effective collisional-radiative recombination and ionization coefficients are calculated for both the optically thin case and a case where all bound-bound uv lines are assumed to be optically thick. These coefficients describe the net recombination and ionization and may be used in sophisticated plasma chemistry simulation codes.

Detailed results are presented showing the deviation of all population densities for all states within our model from those expected if Saha equilibrium conditions were satisfied. It has been shown that for electron densities greater than 6.0×10^{18} cm^{-3} a state of complete local thermodynamic equilibrium exists whereas exited states may be in equilibrium, collision-dominated, for electron densities as low as 2.0×10^{18} cm^{-3}. Coupled to the results for a nitrogen plasma this has implications for simplifying the description of radiative transfer in heated air, in the manner discussed in references [1,2].

V. ACKNOWLEDGMENT

This work was supported by DARPA.

TABLE 1

Energy Levels for O I

Index	State	Configuration($1s^2 2s^2$)	Energy(eV)	Weight
1	^3P	$2p^4$	0.01	9
2	^1D	$2p^4$	1.97	5
3	^1S	$2p^4$	4.19	1
4	$^5S^o$	$2p^3(^4S^o)3s$	9.15	5
5	$^3S^o$	$2p^3(^4S^o)3s$	9.52	3
6	^5P	$2p^3 3p$	10.74	15
7	^3P	$2p^3 3p$	10.99	9
8	$^5S^o$	$2p^3(^4S^o)4s$	11.84	5
9	$^3S^o$	$2p^3(^4S^o)4s$	11.93	3
10	$^5D^o$	$2p^3(^4S^o)3d$	12.08	25
11	$^3D^o$	$2p^3(^4S^o)3d$	12.09	15
12	^5P	$2p^3(^4S^o)4p$	12.29	15
13	^3P	$2p^3(^4S^o)4p$	12.36	9
14	$^3D^o$	$2p^3(^2D^o)3s$	12.54	15
15	$^5S^o$	$2p^3(^4S^o)5s$	12.66	5
16	$^3S^o$	$2p^3(^4S^o)5s$	12.70	3
17	$^1D^o$	$2p^3(^2D^o)3s$	12.73	5

TABLE 2

Energy Levels for O II

Index	State	Configuration($1s^2$)	Energy(eV)	Weight
1	$^4S^o$	$2s^22p^3$	0.0	4
2	$^2D^o$	$2s^22p^3$	3.32	10
3	$^2P^o$	$2s^22p^3$	5.02	6
4	^4P	$2s2p^4$	14.87	12
5	^2D	$2s2p^4$	20.58	10
6	^4P	$2s^22p^2(^3P)3s$	22.99	12
7	^2P	$2s^22p^2(^3P)3s$	23.43	6
8	^2S	$2s2p^4$	24.26	2
9	$^2S^o$	$2s^22p^2(^3P)3p$	25.28	2
10	$^4D^o$	$2s^22p^2(^3P)3p$	25.65	20
11	^2D	$2s^22p^2(^1D)3s$	25.66	10
12	$^4P^o$	$2s^22p^2(^3P)3p$	25.84	12
13	$^2D^o$	$2s^22p^2(^3P)3p$	26.24	10
14	$^4S^o$	$2s^22p^2(^3P)3p$	26.30	4
15	$^2P^o$	$2s^22p^2(^3P)3p$	26.56	6

TABLE 3

Energy Levels for O III

Index	State	Configuration($1s^2$)	Energy(eV)	Weight
1	^3P	$2s^22p^2$	0.0	9
2	$^3D^o$	$2s2p^3$	14.86	15

TABLE 4

Radiative Transitions (Bound-Bound)

Wavelength(Å)	#(Ref.[7])	Spectrum	Index	Energy(eV)
539.4	5	uv	6+ - 1+	22.99
555.1	8	uv	11+ - 2+	22.34
600.6	9	uv	11+ - 3+	20.64
616.6	6	uv	7+ - 2+	20.11
644.2	4	uv	8+ - 3+	19.24
673.2	7	uv	7+ - 3+	18.41
718.5	2	uv	5+ - 2+	17.26
796.7	3	uv	5+ - 3+	15.56
833.8	1	uv	4+ - 1+	14.87
989.5	3	uv	14 - 1	12.53
1026.6	8	uv	11 - 1	12.08
1152.2	4	uv	17 - 2	10.76
1303.5	2	uv	5 - 1	9.51
3735.9	73	uv	14+ - 6+	3.31
3947.3	25	vis	12 - 4	3.14
3966.9	30	vis	15+ - 7+	3.13
4341.3	79	vis	12+ - 6+	2.85
4368.3	26	vis	13 - 5	2.84
4418.1	28	vis	13+ - 7+	2.81
4651.5	23	vis	10+ - 6+	2.66
6455.0	37	vis	15 - 6	1.92
6694.4	75	vis	9+ - 7+	1.85
7254.4	38	vis	16 - 7	1.71
7773.4	11	ir	6 - 4	1.59
7989.9	27	ir	14 - 7	1.55
8446.5	12	ir	7 - 5	1.47
9263.9	28	ir	10 - 6	1.34
11287.0	29	ir	11 - 7	1.10
11299.0	30	ir	8 - 6	1.10
13164.0	31	ir	9 - 7	0.94

TABLE 5

Radiative Transitions (Free-Bound Thresholds)

Wavelength(Å)	Spectrum	Index	Energy(eV)
353.2	uv	1++ - 1+	35.10
353.32	uv	2++ - 4+	35.09
390.12	uv	1++ - 2+	31.78
412.17	uv	1++ - 3+	30.08
421.99	uv	2++ - 5+	29.38
482.41	uv	2++ - 8+	25.70
665.49	uv	3+ - 1	18.63
732.31	uv	2+ - 1	16.93
743.73	uv	3+ - 2	16.67
828.19	uv	2+ - 2	14.97
857.99	uv	3+ - 3	14.45
910.95	uv	1+ - 1	13.61
1023.78	uv	1++ - 6+	12.11
1062.38	uv	1++ - 7+	11.67
1262.53	uv	1++ - 9+	9.82
1311.96	uv	1++ - 10+	9.45
1313.35	uv	1++ - 11+	9.44
1338.88	uv	1++ - 12+	9.26
1399.32	uv	1++ - 13+	8.86
1408.86	uv	1++ - 14+	8.80
1451.76	uv	1++ - 15+	8.54
2773.60	uv	1+ - 4	4.47
2817.73	uv	2+ - 14	4.40
2944.89	uv	2+ - 17	4.21
3023.90	uv	1+ - 5	4.10
4304.86	vis	1+ - 6	2.88
4714.07	vis	1+ - 7	2.63

TABLE 5 (Cont'd)

Radiative Transitions (Free-Bound Thresholds)

Wavelength(Å)	Spectrum	Index	Energy(eV)
6965.17	vis	1+ - 8	1.78
7336.09	vis	1+ - 9	1.69
8050.65	ir	1+ - 10	1.54
8103.27	ir	1+ - 11	1.53
9321.80	ir	1+ - 12	1.33
9839.69	ir	1+ - 13	1.26
12914.58	ir	1+ - 15	0.96
13476.09	ir	1+ - 16	0.92

TABLE 6

Collisional-Radiative Recombination Coefficients

Optically Thin (All Wavelengths)

Neutral

Te(eV)	1.0	1.5	2.0	2.5	3.0
Ne					
1.0E+16	1.8E-11	6.8E-12	4.4E-12	3.0E-12	1.5E-12
2.0	3.0	1.3E-11	7.9	5.1	2.8
3.0	4.1	1.8	1.2E-11	7.4	4.1
4.0	5.2	2.4	1.5	9.9	5.3
5.0	6.4	3.0	1.9	1.2E-11	6.5
6.0	7.5	3.6	2.3	1.4	7.8
7.0	8.6	4.1	2.6	1.7	9.1
8.0	9.7	4.7	3.0	1.9	1.0E-11
9.0	1.1E-10	5.4	3.4	2.2	1.2
1.0E+17	1.2	6.5	3.7	2.4	1.3
2.0	2.3	1.2E-10	7.6	4.8	3.0
3.0	3.5	1.8	1.1E-10	7.4	4.4
4.0	4.6	2.4	1.5	9.8	6.0
5.0	5.8	3.0	1.9	1.2E-10	7.7
6.0	7.0	3.6	2.2	1.5	9.4
7.0	8.1	4.2	2.6	1.7	1.1E-10
8.0	9.3	4.9	3.0	2.0	1.3
9.0	1.0E-09	5.5	3.4	2.2	1.4
1.0E+18	1.2	6.1	3.7	2.5	1.6
2.0	2.3	1.2E-09	7.4	4.9	3.3
3.0	3.5	1.9	1.1E-09	7.4	5.1
4.0	4.7	2.5	1.5	1.0E-09	6.9
5.0	5.9	3.1	1.9	1.2	8.6
6.0	7.1	3.8	2.2	1.5	1.0E-09
7.0	8.2	4.4	2.6	1.7	1.2
8.0	9.6	5.0	3.0	2.0	1.4
9.0	1.1E-08	5.7	3.4	2.2	1.6
1.0E+19	1.2	6.3	3.8	2.5	1.7

TABLE 7

Collisional-Radiative Recombination Coefficients

Optically Thin (All Wavelengths)

Ion

Te(eV)	1.0	1.5	2.0	2.5	3.0
Ne					
1.0E+16	3.2E-12	2.0E-12	1.6E-12	1.5E-12	1.1E-12
2.0	3.4	2.2	1.8	1.6	1.2
3.0	3.7	2.4	2.0	1.7	1.3
4.0	4.0	2.7	2.2	1.9	1.4
5.0	4.4	2.9	2.4	2.0	1.5
6.0	4.7	3.2	2.6	2.2	1.5
7.0	5.0	3.4	2.8	2.3	1.6
8.0	5.4	3.6	3.0	2.5	1.7
9.0	5.7	3.9	3.2	2.6	1.9
1.0E+17	6.0	4.5	3.4	2.9	2.0
2.0	9.6	6.7	5.5	4.4	3.3
3.0	1.4E-11	9.2	7.4	6.1	4.4
4.0	1.7	1.2E-11	9.3	7.6	5.7
5.0	2.1	1.4	1.1E-11	9.3	7.0
6.0	2.5	1.7	1.3	1.1E-11	8.3
7.0	2.9	1.9	1.5	1.3	9.6
8.0	3.3	2.2	1.7	1.4	1.1E-11
9.0	3.6	2.5	1.9	1.6	1.2
1.0E+18	4.0	2.7	2.1	1.7	1.3
2.0	7.9	5.3	4.1	3.4	2.7
3.0	1.2E-10	8.0	6.0	5.0	4.1
4.0	1.6	1.1E-10	8.1	6.6	5.4
5.0	2.0	1.3	1.0E-10	8.4	6.8
6.0	2.4	1.6	1.2	1.0E-10	8.2
7.0	2.7	1.8	1.4	1.1	9.5
8.0	3.1	2.1	1.6	1.3	1.1E-10
9.0	3.5	2.4	1.8	1.5	1.2
1.0E+19	3.8	2.6	2.0	1.7	1.4

TABLE 8

Collisional-Radiative Ionization Coefficients

Optically Thin (All Wavelengths)

Neutral

Te(eV)	1.0	1.5	2.0	2.5	3.0
Ne					
1.0E+16	2.9E-13	2.7E-11	3.1E-10	1.0E-09	2.1E-09
2.0	4.3	4.7	5.2	1.9	3.6
3.0	5.6	6.5	7.3	2.7	5.1
4.0	6.8	8.1	9.0	3.4	6.3
5.0	8.0	9.6	1.1E-09	4.0	7.4
6.0	9.1	1.1E-10	1.2	4.5	8.4
7.0	1.0E-12	1.2	1.4	5.1	9.4
8.0	1.1	1.4	1.5	5.5	1.0E-08
9.0	1.2	1.5	1.6	6.0	1.1
1.0E+17	1.3	1.7	1.7	6.4	1.2
2.0	2.0	2.3	2.4	9.0	1.9
3.0	2.5	2.8	2.8	1.1E-08	2.2
4.0	2.8	3.1	3.1	1.2	2.4
5.0	3.1	3.3	3.3	1.2	2.6
6.0	3.3	3.4	3.4	1.3	2.7
7.0	3.5	3.6	3.5	1.3	2.8
8.0	3.6	3.7	3.6	1.3	2.9
9.0	3.8	3.8	3.7	1.4	3.0
1.0E+18	3.9	3.9	3.8	1.4	3.0
2.0	4.7	4.3	4.1	1.5	3.3
3.0	5.1	4.6	4.3	1.6	3.5
4.0	5.5	4.8	4.4	1.6	3.6
5.0	5.9	5.0	4.5	1.6	3.6
6.0	6.2	5.1	4.6	1.7	3.7
7.0	6.4	5.3	4.7	1.7	3.7
8.0	6.6	5.4	4.8	1.7	3.8
9.0	6.9	5.5	4.9	1.7	3.8
1.0E+19	7.1	5.6	4.9	1.7	3.8

TABLE 9

Collisional-Radiative Ionization Coefficients

Optically Thin (All Wavelengths)

Ion

Te(eV)	1.0	1.5	2.0	2.5	3.0
Ne					
1.0E+16	2.7E-23	2.5E-18	8.2E-16	2.3E-14	2.2E-13
2.0	3.0	2.9	9.5	2.9	2.5
3.0	3.5	3.3	1.1E-15	3.4	2.8
4.0	3.9	3.8	1.2	3.8	3.1
5.0	4.4	4.2	1.4	4.1	3.4
6.0	4.8	4.7	1.5	4.5	3.7
7.0	5.2	5.1	1.6	4.9	3.9
8.0	5.6	5.5	1.8	5.3	4.2
9.0	6.0	6.0	1.9	5.7	4.5
1.0E+17	6.4	6.9	2.0	6.1	4.8
2.0	1.0E-22	1.0E-17	3.2	9.3	8.0
3.0	1.3	1.3	4.1	1.2E-13	1.0E-12
4.0	1.6	1.6	4.8	1.5	1.3
5.0	1.8	1.8	5.5	1.7	1.5
6.0	2.0	2.0	6.1	1.8	1.7
7.0	2.2	2.2	6.6	2.0	1.8
8.0	2.4	2.3	7.0	2.1	1.9
9.0	2.5	2.5	7.4	2.3	2.1
1.0E+18	2.6	2.6	7.8	2.4	2.2
2.0	3.7	3.5	1.0E-14	3.1	2.9
3.0	4.5	4.0	1.2	3.5	3.4
4.0	5.2	4.5	1.3	3.8	3.6
5.0	5.8	4.8	1.4	4.0	3.8
6.0	6.4	5.1	1.4	4.2	4.0
7.0	7.0	5.4	1.5	4.4	4.1
8.0	7.6	5.7	1.6	4.5	4.2
9.0	8.1	6.0	1.7	4.6	4.3
1.0E+19	8.6	6.2	1.7	4.7	4.4

TABLE 10

Collisional-Radiative Recombination Coefficients

Optically Thick (All Bound-Bound UV Wavelengths)

Neutral

Te(eV)	1.0	1.5	2.0	2.5	3.0
Ne					
1.0E+16	1.8E-11	6.9E-12	4.2E-12	1.8E-12	1.0E-12
2.0	3.0	1.3E-11	7.9	3.8	2.0
3.0	4.1	1.8	1.2E-11	5.8	3.1
4.0	5.3	2.4	1.5	7.7	4.3
5.0	6.4	3.0	1.9	9.7	5.4
6.0	7.5	3.6	2.3	1.2E-11	6.6
7.0	8.6	4.2	2.6	1.4	7.8
8.0	9.6	4.8	3.0	1.6	8.9
9.0	1.1E-10	5.4	3.4	1.8	1.0E-11
1.0E+17	1.2	6.1	3.7	2.1	1.1
2.0	2.3	1.2E-10	7.6	4.5	2.5
3.0	3.4	1.8	1.1E-10	7.0	3.9
4.0	4.6	2.4	1.5	9.5	5.6
5.0	5.8	3.0	1.9	1.2E-10	7.3
6.0	7.0	3.7	2.2	1.4	9.0
7.0	8.2	4.3	2.6	1.7	1.1E-10
8.0	9.4	4.9	3.0	1.9	1.2
9.0	1.0E-09	5.5	3.3	2.2	1.4
1.0E+18	1.2	6.1	3.7	2.5	1.6
2.0	2.4	1.2E-09	7.4	4.9	3.3
3.0	3.5	1.9	1.1E-09	7.4	5.1
4.0	4.7	2.5	1.5	9.9	6.9
5.0	5.9	3.2	1.9	1.2E-09	8.7
6.0	7.1	3.8	2.3	1.5	1.0E-09
7.0	8.2	4.4	2.6	1.7	1.2
8.0	9.4	5.0	3.0	2.0	1.4
9.0	1.0E-08	5.7	3.4	2.2	1.6
1.0E+19	1.2	6.3	3.8	2.5	1.8

TABLE 11

Collisional-Radiative Recombination Coefficients

Optically Thick (All Bound-Bound UV Wavelengths)

Te(eV)	Ion 1.0	1.5	2.0	2.5	3.0
Ne					
1.0E+16	3.1E-12	2.0E-12	1.7E-12	1.2E-12	8.2E-13
2.0	3.5	2.2	1.8	1.3	9.6
3.0	3.8	2.5	2.0	1.4	1.1E-12
4.0	4.0	2.7	2.2	1.6	1.2
5.0	4.4	2.9	2.4	1.7	1.3
6.0	4.7	3.2	2.6	1.9	1.4
7.0	5.0	3.4	2.8	2.0	1.5
8.0	5.3	3.7	3.0	2.2	1.6
9.0	5.8	3.9	3.2	2.3	1.7
1.0E+17	6.0	4.2	3.4	2.5	1.8
2.0	9.9	6.8	5.5	4.1	2.9
3.0	1.3E-11	9.3	7.4	5.8	4.1
4.0	1.7	1.2E-11	9.3	7.4	5.3
5.0	2.1	1.4	1.1E-11	9.1	6.6
6.0	2.5	1.7	1.3	1.1E-11	8.0
7.0	2.9	2.0	1.5	1.2	9.4
8.0	3.3	2.2	1.7	1.4	1.1E-11
9.0	3.7	2.5	1.9	1.6	1.2
1.0E+18	4.0	2.7	2.1	1.7	1.4
2.0	8.0	5.3	4.1	3.4	2.7
3.0	1.2E-10	8.0	5.8	5.0	4.1
4.0	1.6	1.1E-10	8.1	6.7	5.5
5.0	2.0	1.3	1.0E-10	8.4	6.8
6.0	2.3	1.6	1.2	1.0E-10	8.2
7.0	2.7	1.9	1.4	1.1	9.5
8.0	3.1	2.1	1.6	1.3	1.1E-10
9.0	3.5	2.4	1.8	1.5	1.2
1.0E+19	3.9	2.7	2.0	1.7	1.4

TABLE 12

Collisional-Radiative Ionization Coefficients

Optically Thick (All Bound-Bound Wavelengths)

Neutral

Te(eV)	1.0	1.5	2.0	2.5	3.0
Ne					
1.0E+16	3.0E-12	9.2E-11	5.8E-10	1.5E-09	2.5E-09
2.0	3.2	1.4E-10	9.5	2.3	4.1
3.0	3.4	1.8	1.3E-09	3.1	5.4
4.0	3.5	2.0	1.5	3.9	6.7
5.0	3.5	2.3	1.7	4.6	8.0
6.0	3.6	2.4	1.9	5.2	9.1
7.0	3.6	2.6	2.1	5.8	1.0E-08
8.0	3.7	2.7	2.2	6.3	1.1
9.0	3.7	2.8	2.3	6.8	1.2
1.0E+17	3.8	2.9	2.4	7.2	1.3
2.0	4.1	3.5	3.1	1.0E-08	1.9
3.0	4.2	3.7	3.4	1.2	2.2
4.0	4.4	3.9	3.6	1.2	2.5
5.0	4.5	4.0	3.7	1.3	2.7
6.0	4.6	4.1	3.8	1.4	2.8
7.0	4.6	4.2	3.9	1.4	2.9
8.0	4.7	4.2	3.9	1.4	2.9
9.0	4.7	4.2	4.0	1.4	3.0
1.0E+18	4.8	4.3	4.0	1.4	3.1
2.0	5.2	4.6	4.3	1.5	3.4
3.0	5.6	4.8	4.3	1.6	3.5
4.0	5.9	5.0	4.5	1.6	3.6
5.0	6.2	5.1	4.6	1.7	3.6
6.0	6.4	5.3	4.7	1.7	3.7
7.0	6.7	5.4	4.8	1.7	3.7
8.0	6.9	5.5	4.8	1.7	3.8
9.0	7.1	5.6	4.9	1.7	3.8
1.0E+19	7.4	5.7	5.0	1.8	3.9

TABLE 13

Collisional-Radiative Ionization Coefficients

Optically Thick (All Bound-Bound UV Wavelengths)

Te(eV)	Ion 1.0	1.5	2.0	2.5	3.0
Ne					
1.0E+16	3.0E-22	3.2E-17	9.9E-15	2.3E-13	1.7E-12
2.0	3.0	3.2	1.0E-14	2.4	1.7
3.0	3.0	3.3	1.1	2.5	1.8
4.0	3.0	3.3	1.1	2.6	1.9
5.0	3.0	3.4	1.1	2.7	1.9
6.0	3.0	3.4	1.1	2.8	2.0
7.0	3.0	3.4	1.1	2.8	2.1
8.0	3.0	3.5	1.1	2.9	2.1
9.0	3.0	3.5	1.1	2.9	2.2
1.0E+17	3.0	3.5	1.1	3.0	2.2
2.0	3.2	3.7	1.2	3.3	2.6
3.0	3.3	3.7	1.2	3.5	2.9
4.0	3.4	3.8	1.2	3.7	3.0
5.0	3.5	3.9	1.2	3.7	3.2
6.0	3.6	3.9	1.3	3.8	3.3
7.0	3.7	4.0	1.3	3.9	3.4
8.0	3.8	4.0	1.3	3.9	3.5
9.0	3.9	4.1	1.3	3.9	3.5
1.0E+18	4.0	4.1	1.3	4.0	3.6
2.0	4.7	4.5	1.4	4.2	3.9
3.0	5.3	4.9	1.4	4.4	4.1
4.0	5.8	5.2	1.5	4.5	4.2
5.0	6.4	5.4	1.6	4.6	4.3
6.0	7.0	5.7	1.6	4.7	4.4
7.0	7.5	5.9	1.6	4.8	4.5
8.0	8.1	6.2	1.7	4.9	4.6
9.0	8.6	6.4	1.7	5.0	4.7
1.0E+19	9.2	6.6	1.8	5.1	4.8

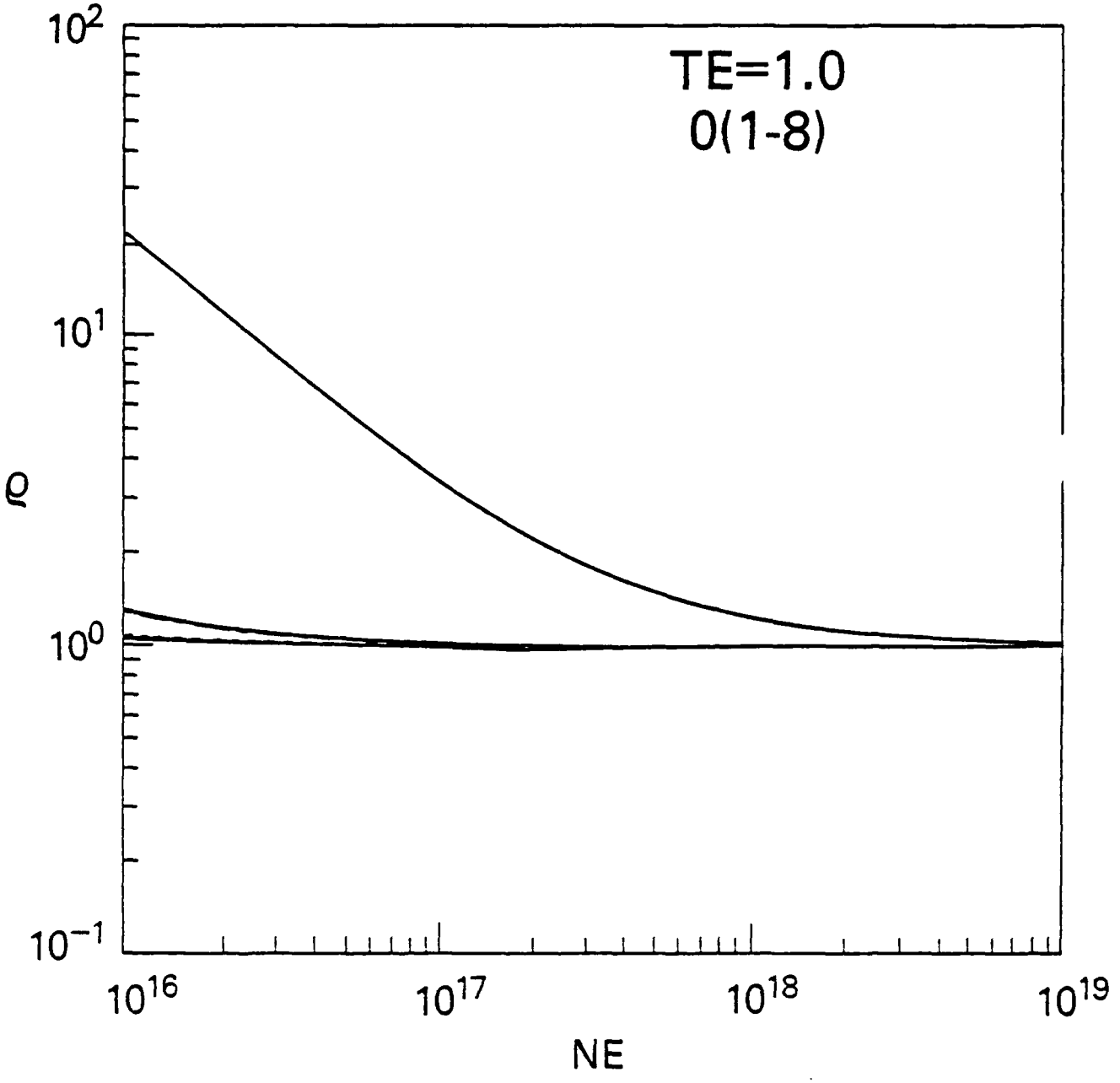

Fig. 1. Saha decrements, Te=1.0 eV. The initial order from top to bottom is ρ(1,2,3), ρ(4,6,8) and ρ(5,7). ρ(1,2,3) denotes ρ(1)=ρ(2)=ρ(3) to the resolution of the figure.

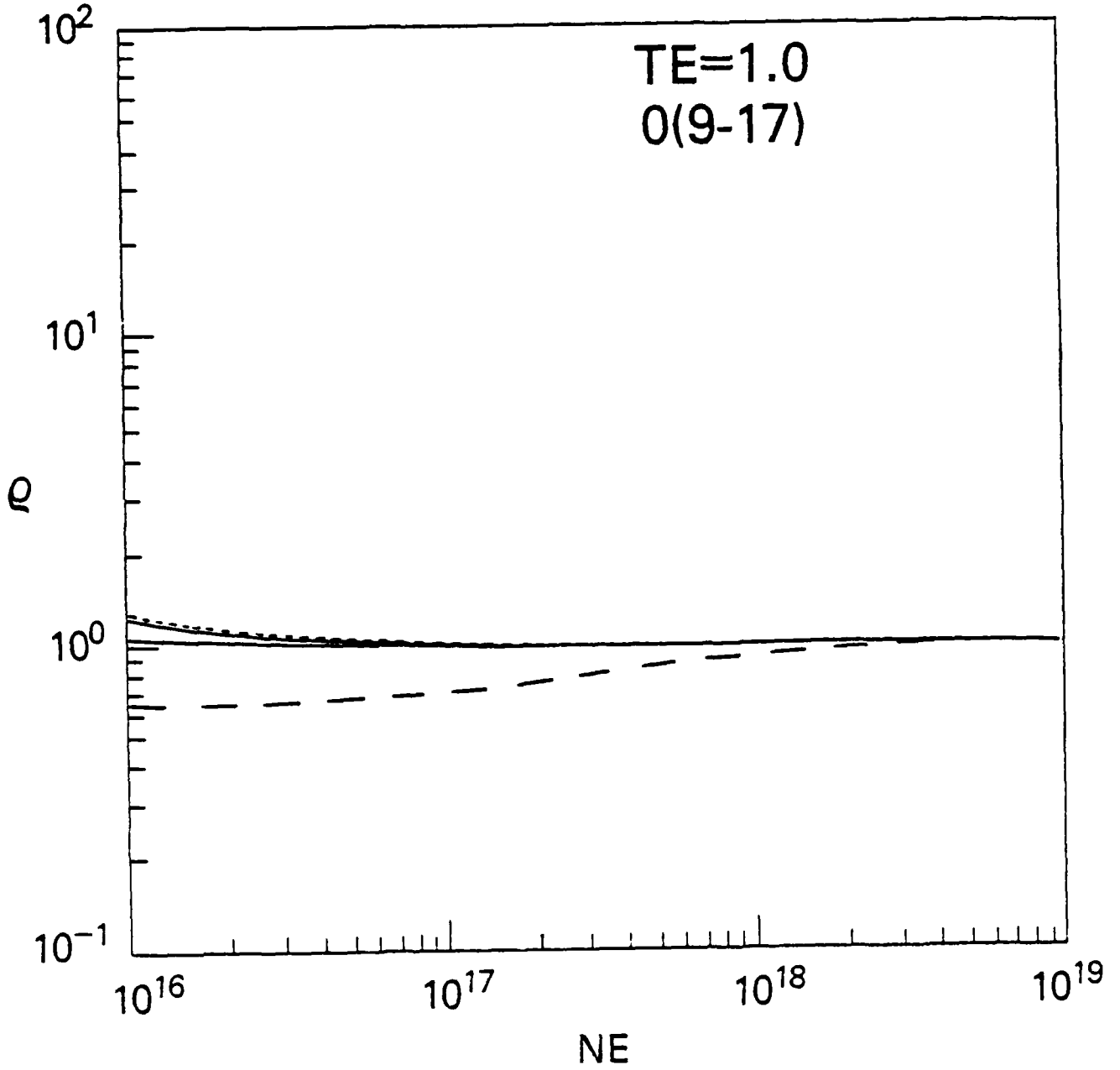

Fig. 2. Saha decrements, Te=1.0 eV. The initial order from top to bottom is ρ(10), ρ(12-16), ρ(9,11) and ρ(17).

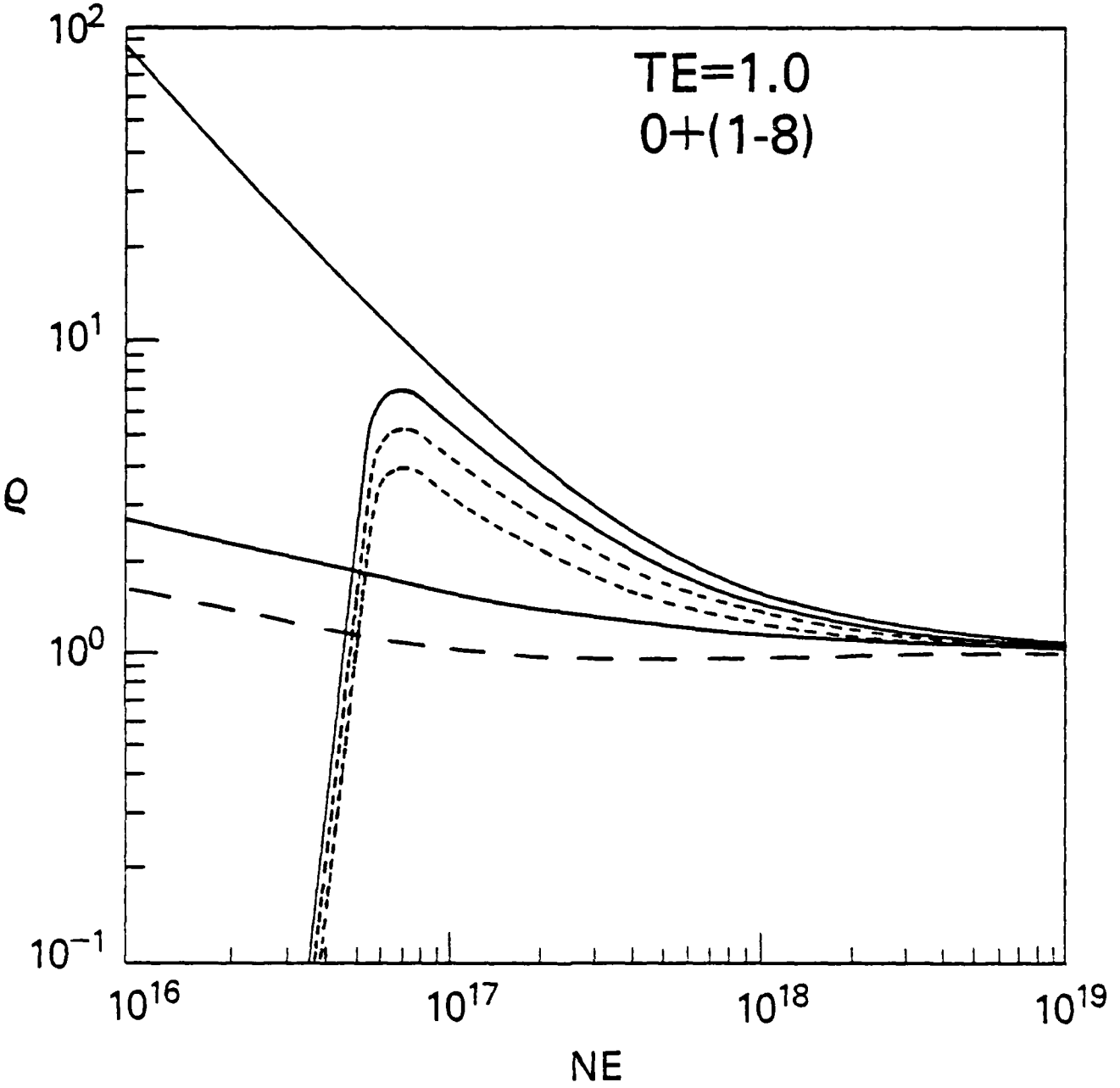

Fig. 3. Saha decrements, Te=1.0 eV. The initial order from top to bottom is $\rho^+(1,2,3)$, $\rho^+(7)$, $\rho^+(6)$, $\rho^+(4)$, $\rho^+(5)$ and $\rho^+(8)$.

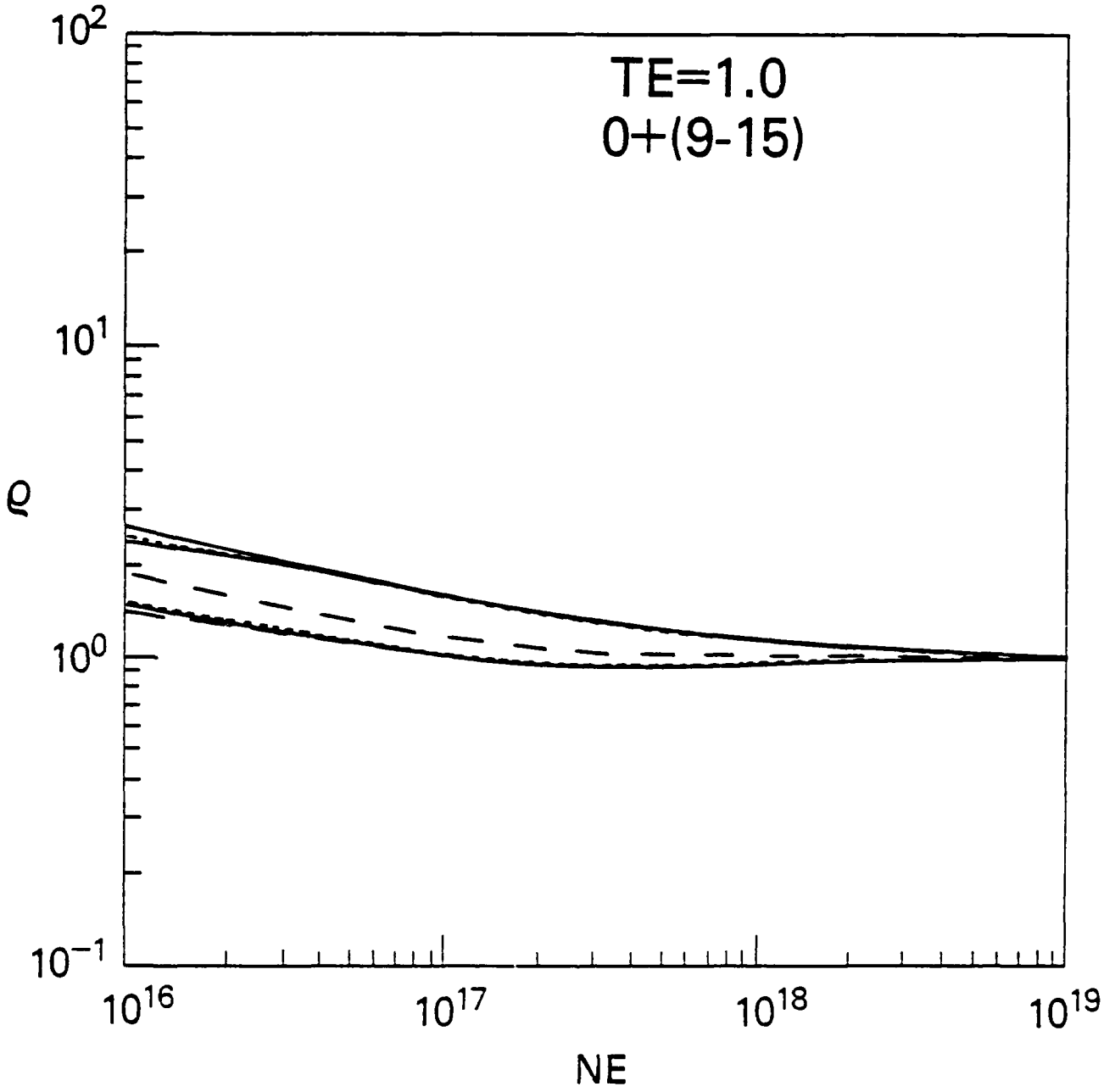

Fig. 4. Saha decrements, Te=1.0 eV. The initial order from top to bottom is $\rho^+(9)$, $\rho^+(13)$, $\rho^+(15)$, $\rho^+(11)$, $\rho^+(10)$, $\rho^+(12)$ and $\rho^+(14)$.

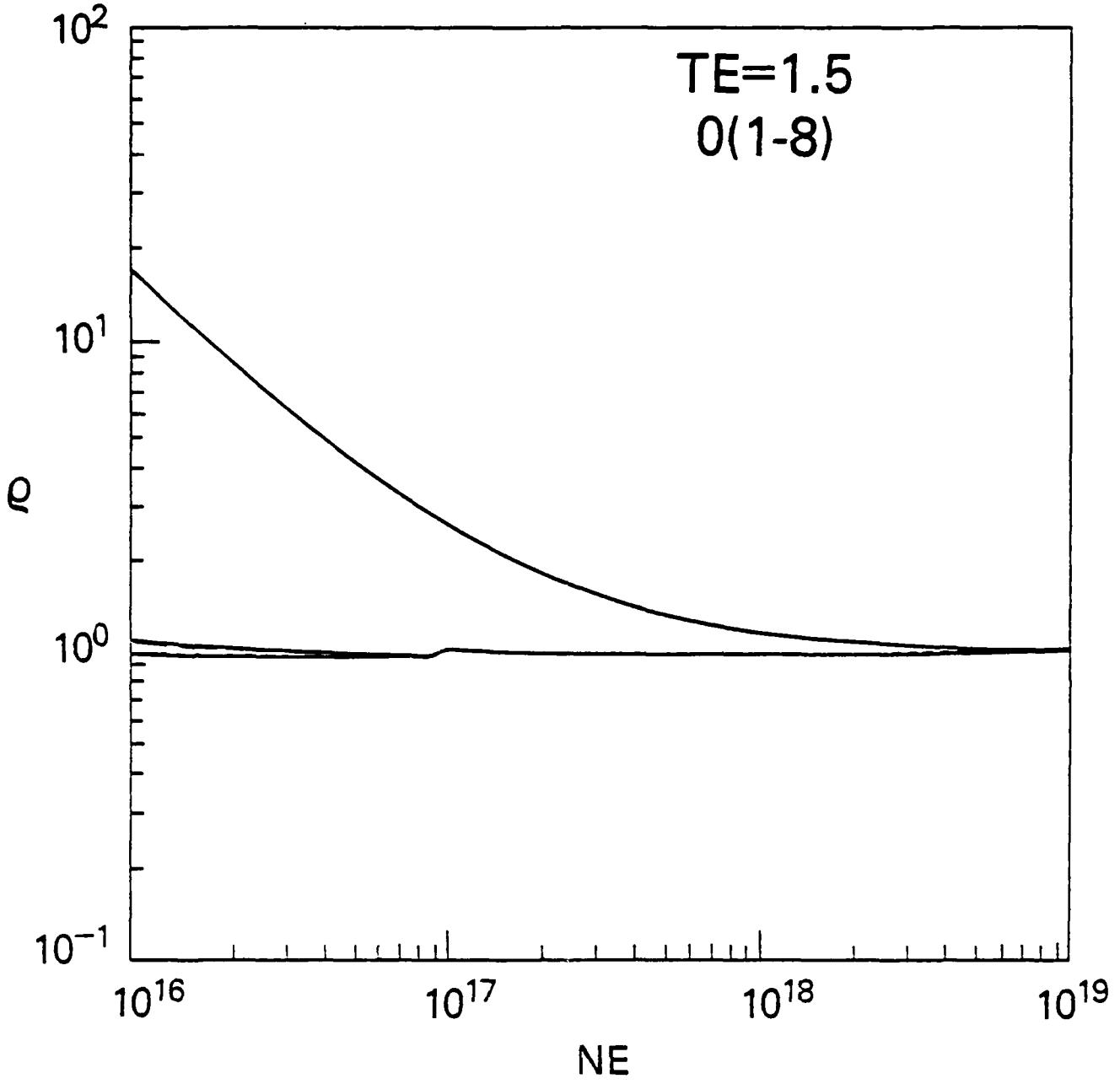

Fig. 5. Saha decrements, Te=1.5 eV; as in Fig. 1.

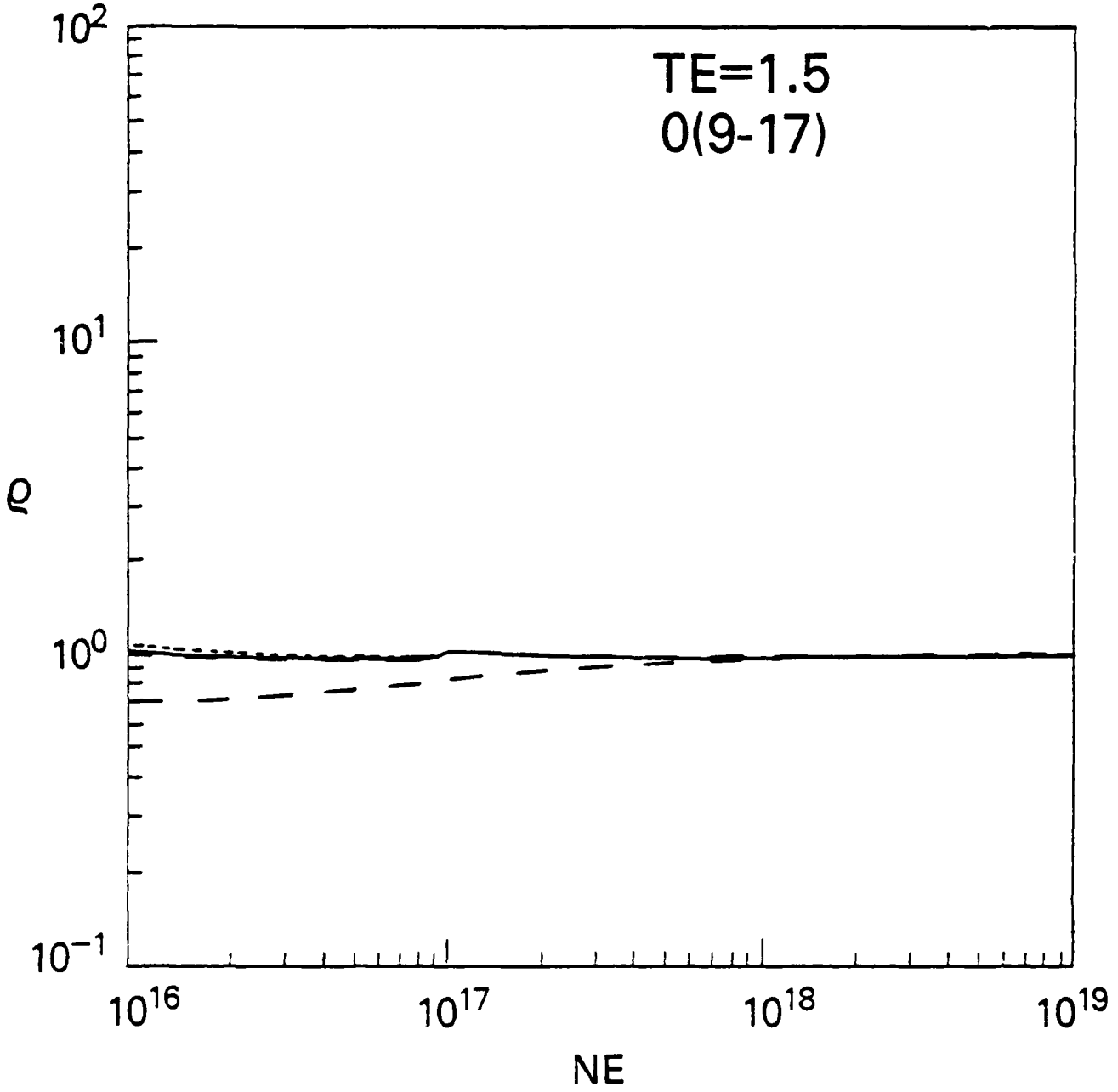

Fig. 6. Saha decrements, Te=1.5 eV. The initial order from top to bottom is ρ(10), ρ(9,11-16) and ρ(17).

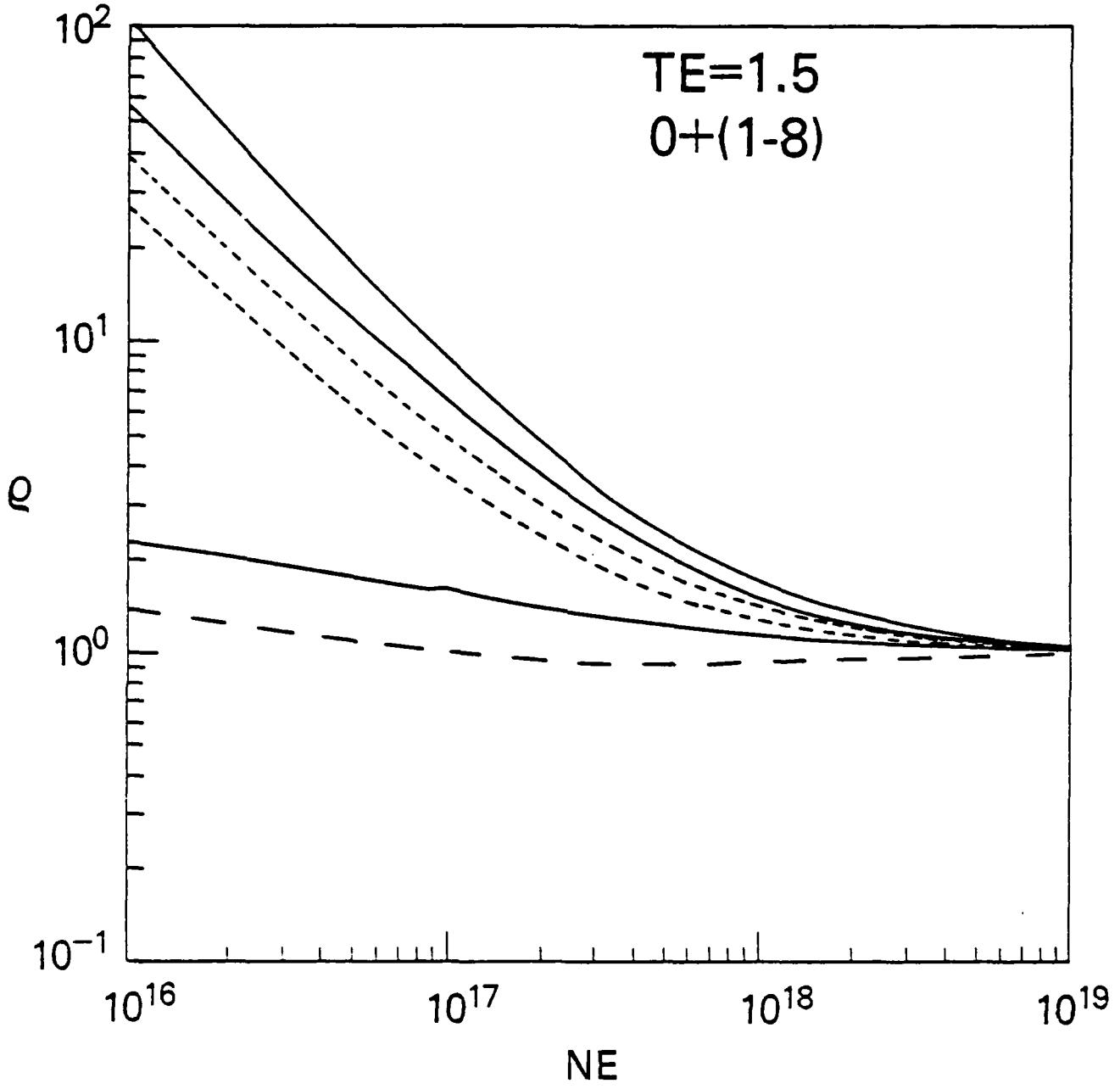

Fig. 7. Saha decrements, Te=1.5 eV. The initial order from top to bottom is $\rho^+(1,2,3)$, $\rho^+(4)$, $\rho^+(5)$, $\rho^+(8)$, $\rho^+(7)$ and $\rho^+(6)$.

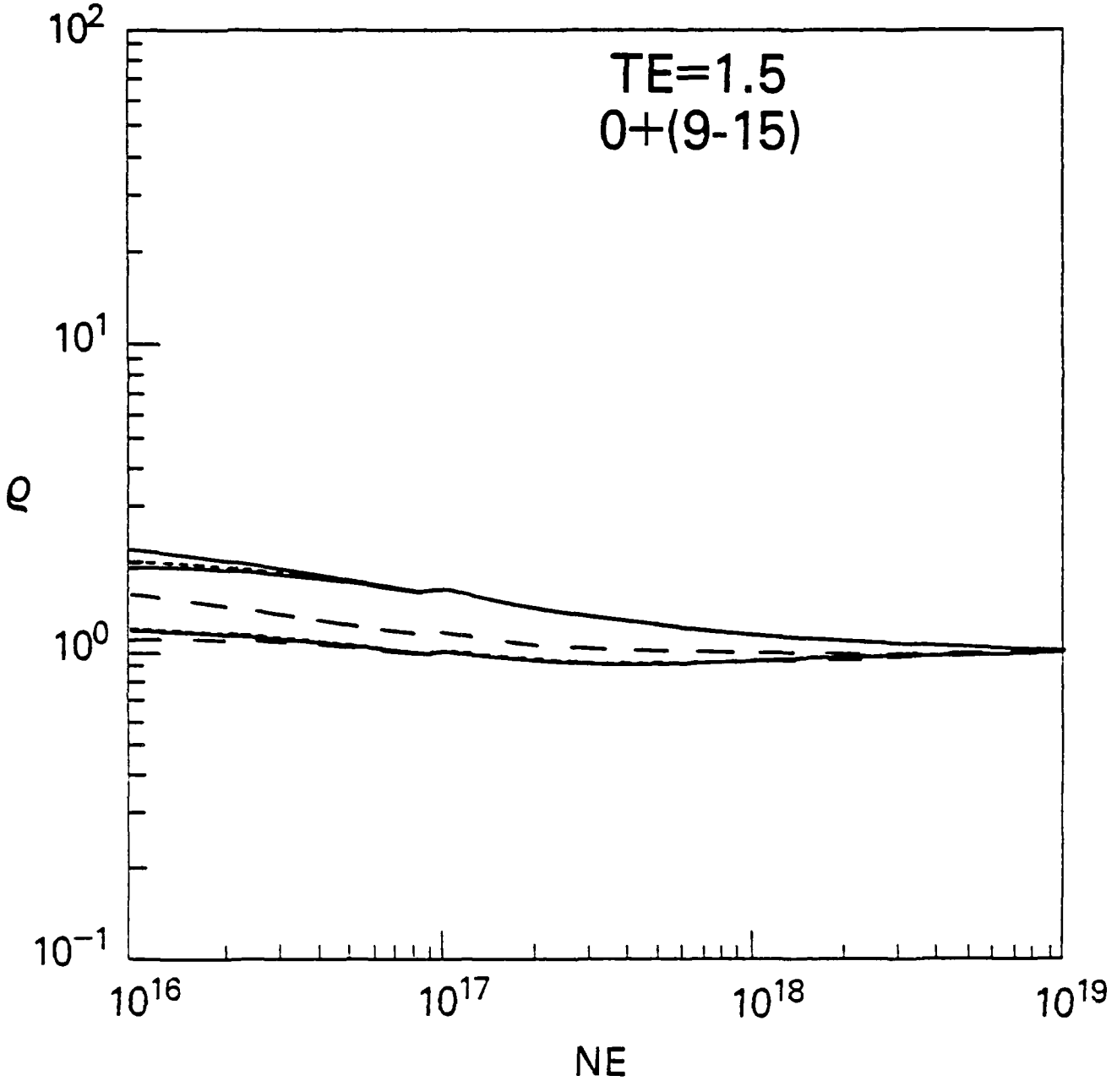

Fig. 8. Saha decrements, Te=1.5 eV. The initial order from top to bottom is $\rho^+(9)$, $\rho^+(13)$, $\rho^+(15)$, $\rho^+(11)$, $\rho^+(10,12)$ and $\rho^+(14)$.

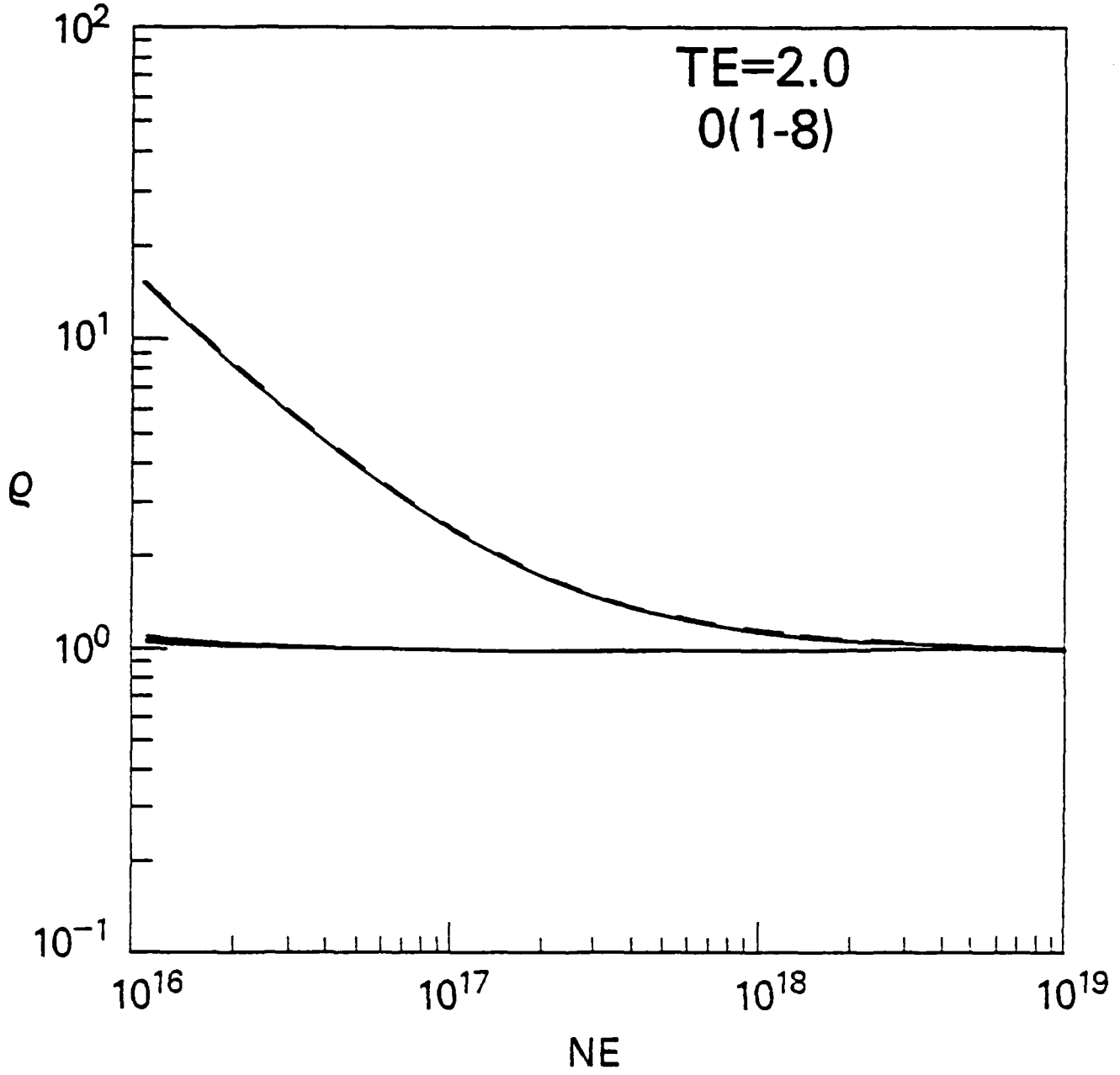

Fig. 9. Saha decrements, Te=2.0 eV. The initial order from top to bottom is ρ(1,2,3) and ρ(4-8).

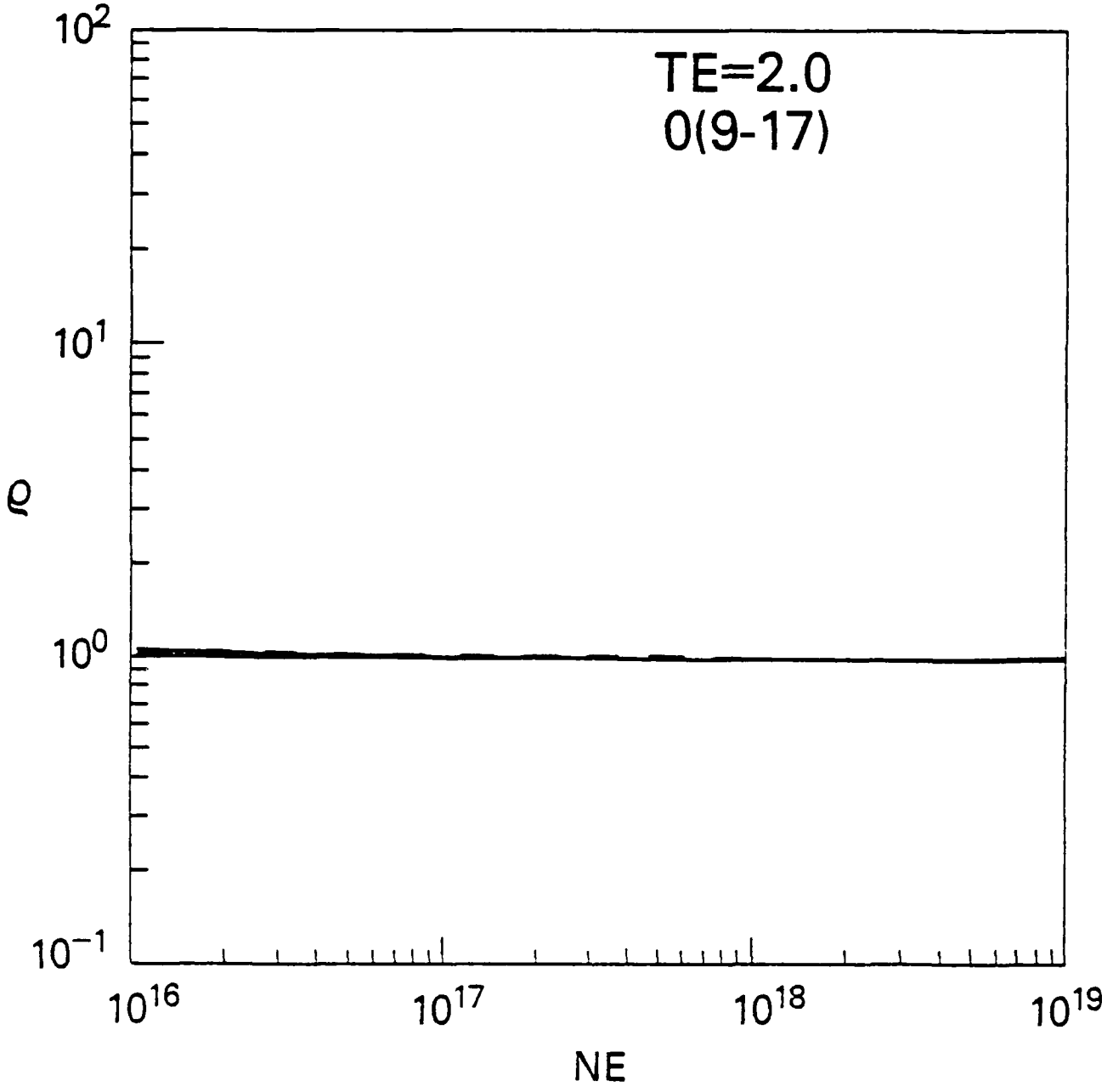

Fig. 10. Saha decrements, Te=2.0 eV. The initial order from top to bottom is ρ(9-17).

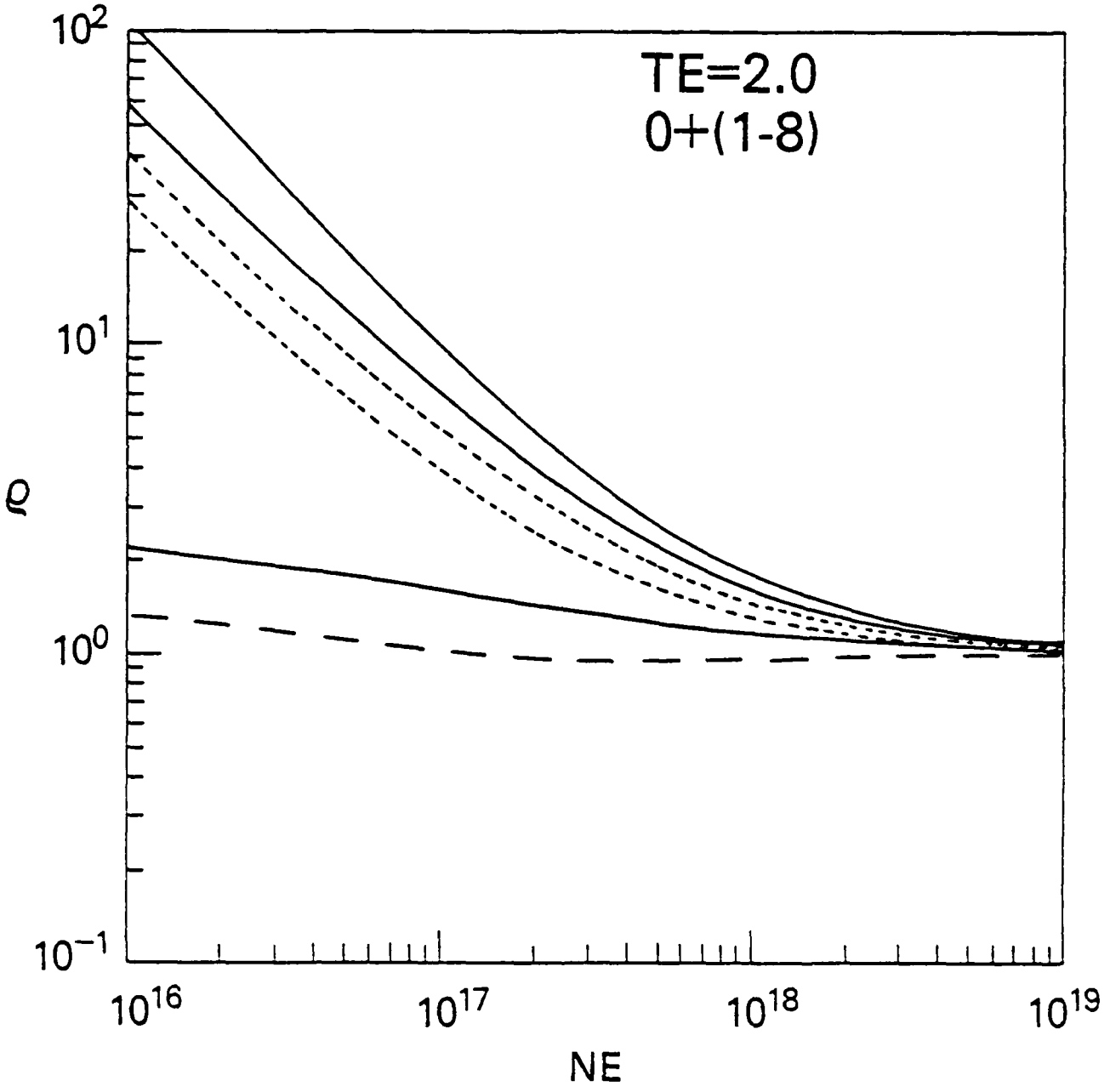

Fig. 11. Saha decrements, Te=2.0 eV; as in Fig. 7.

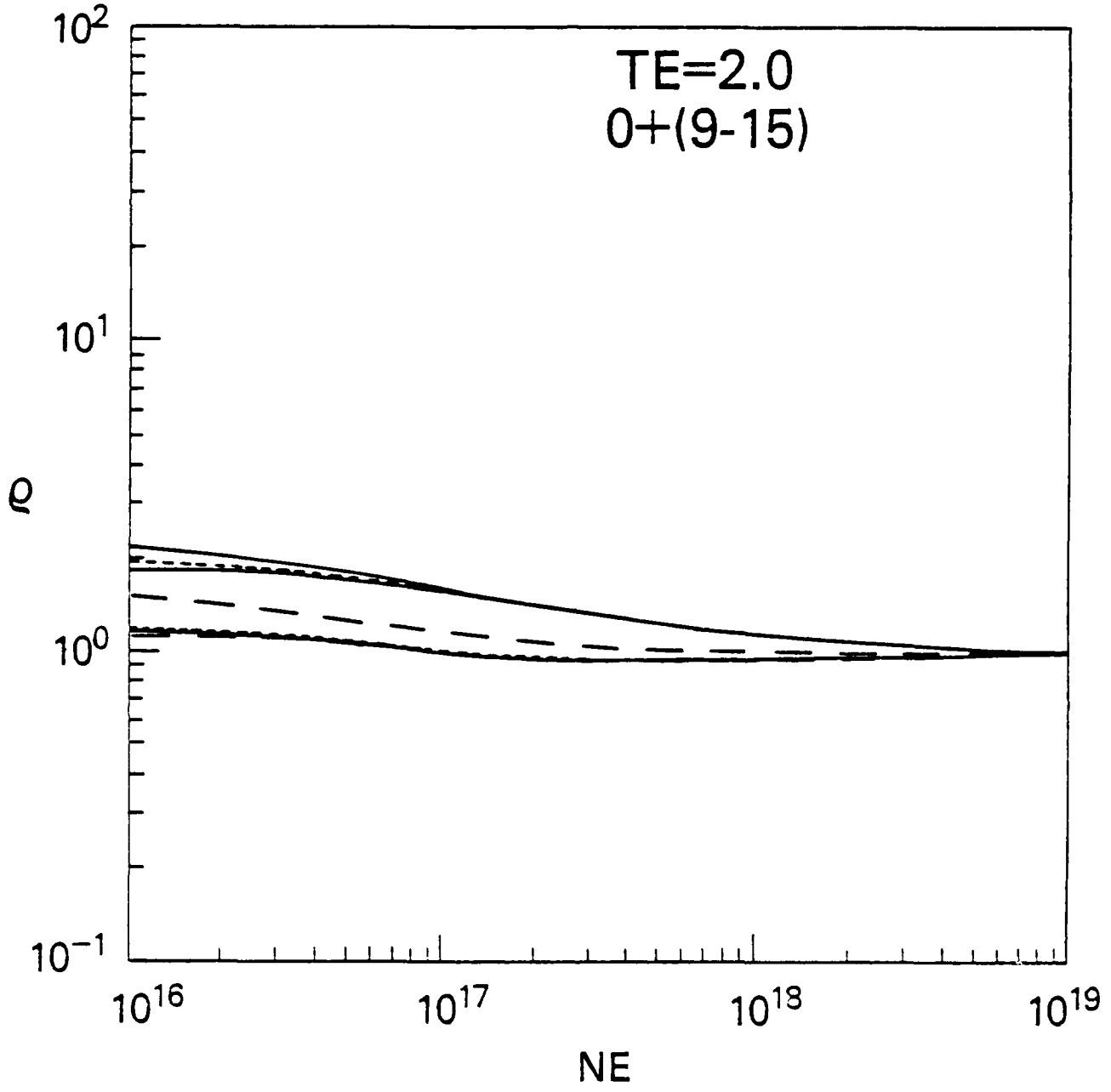

Fig. 12. Saha decrements, Te=2.0 eV; as in Fig. 8.

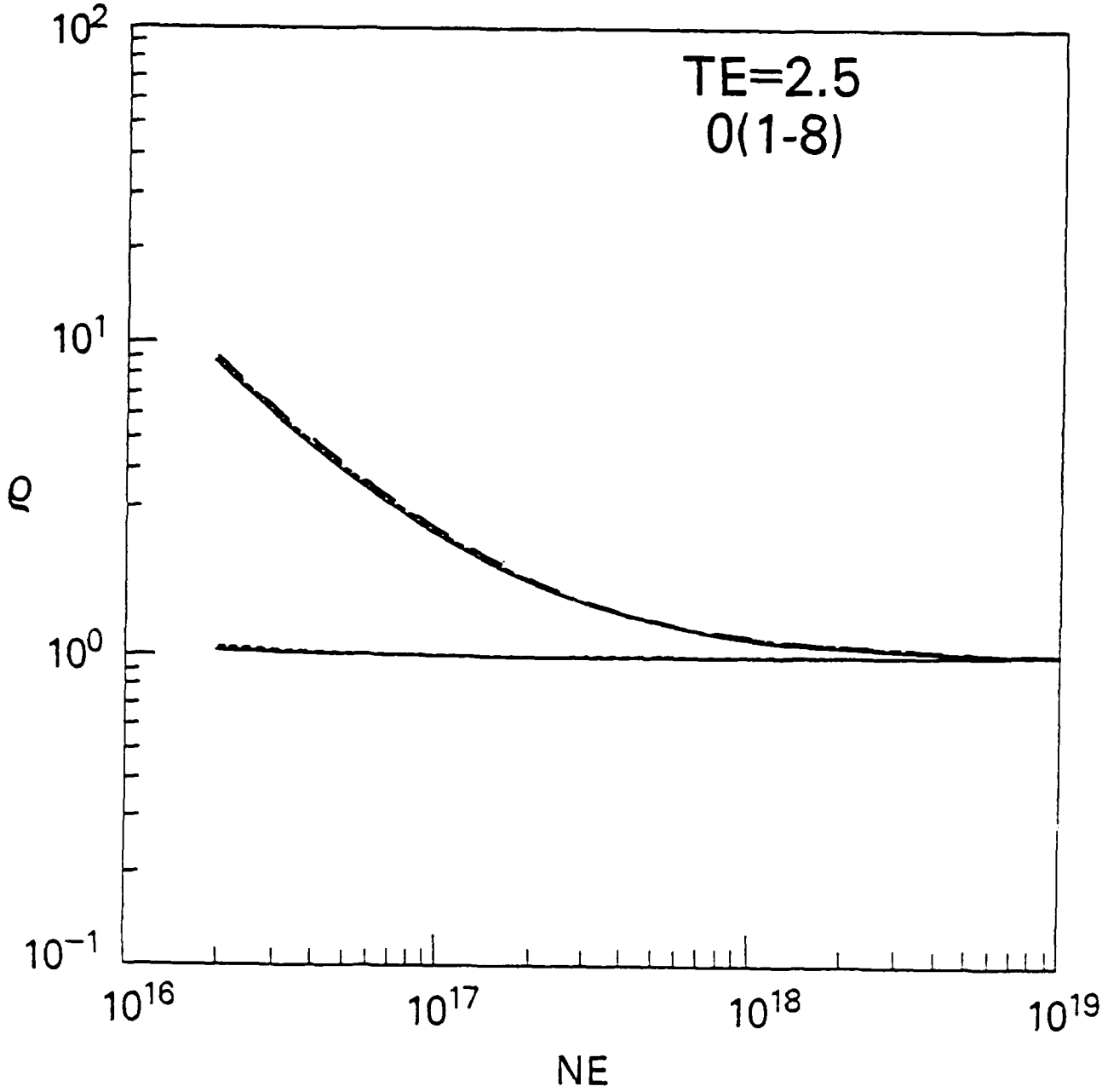

Fig. 13. Saha decrements, Te=2.5 eV; as in Fig. 9.

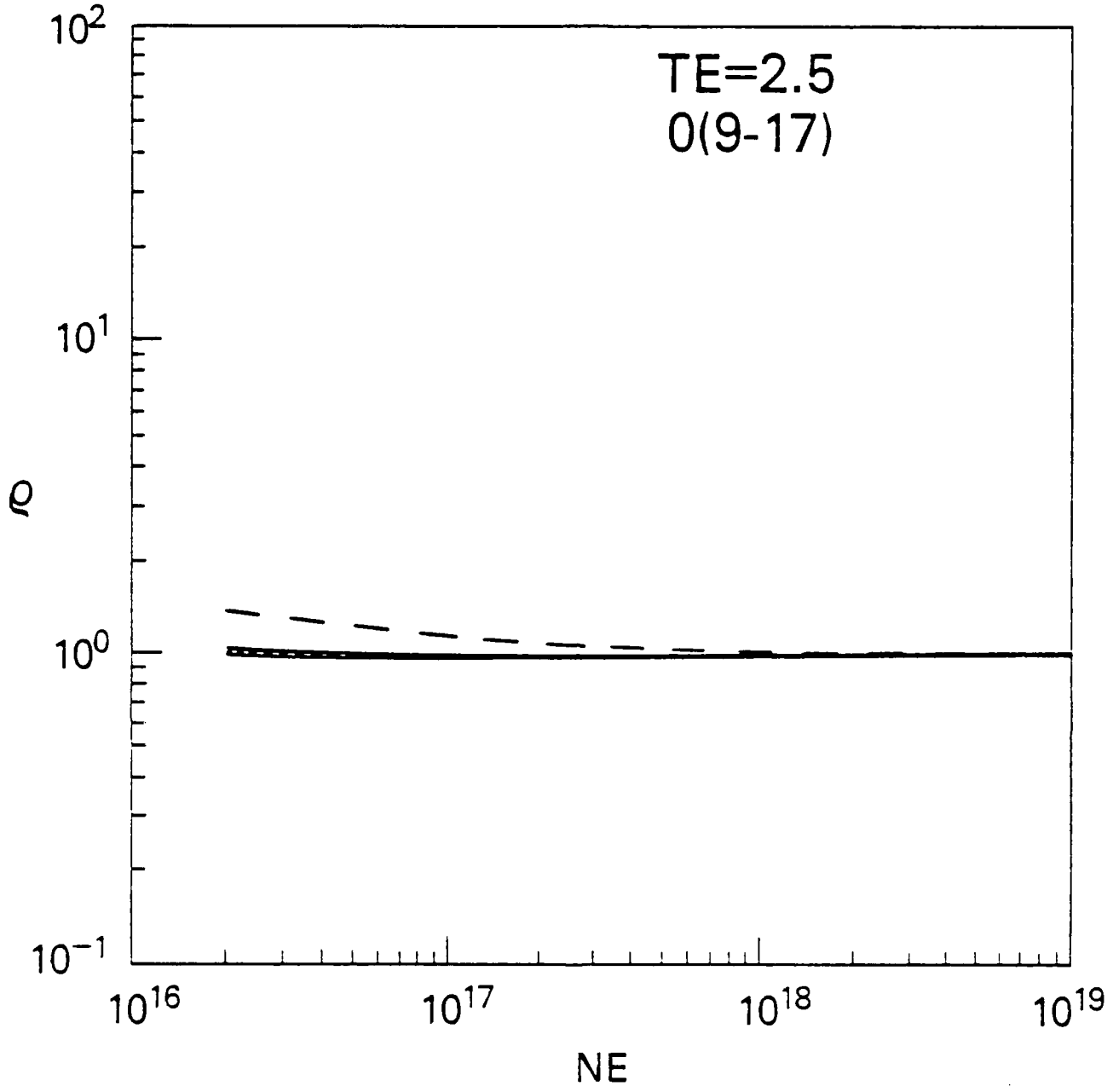

Fig. 14. Saha decrements, Te=2.5 eV. The initial order from top to bottom is ρ(17) and ρ(9-16).

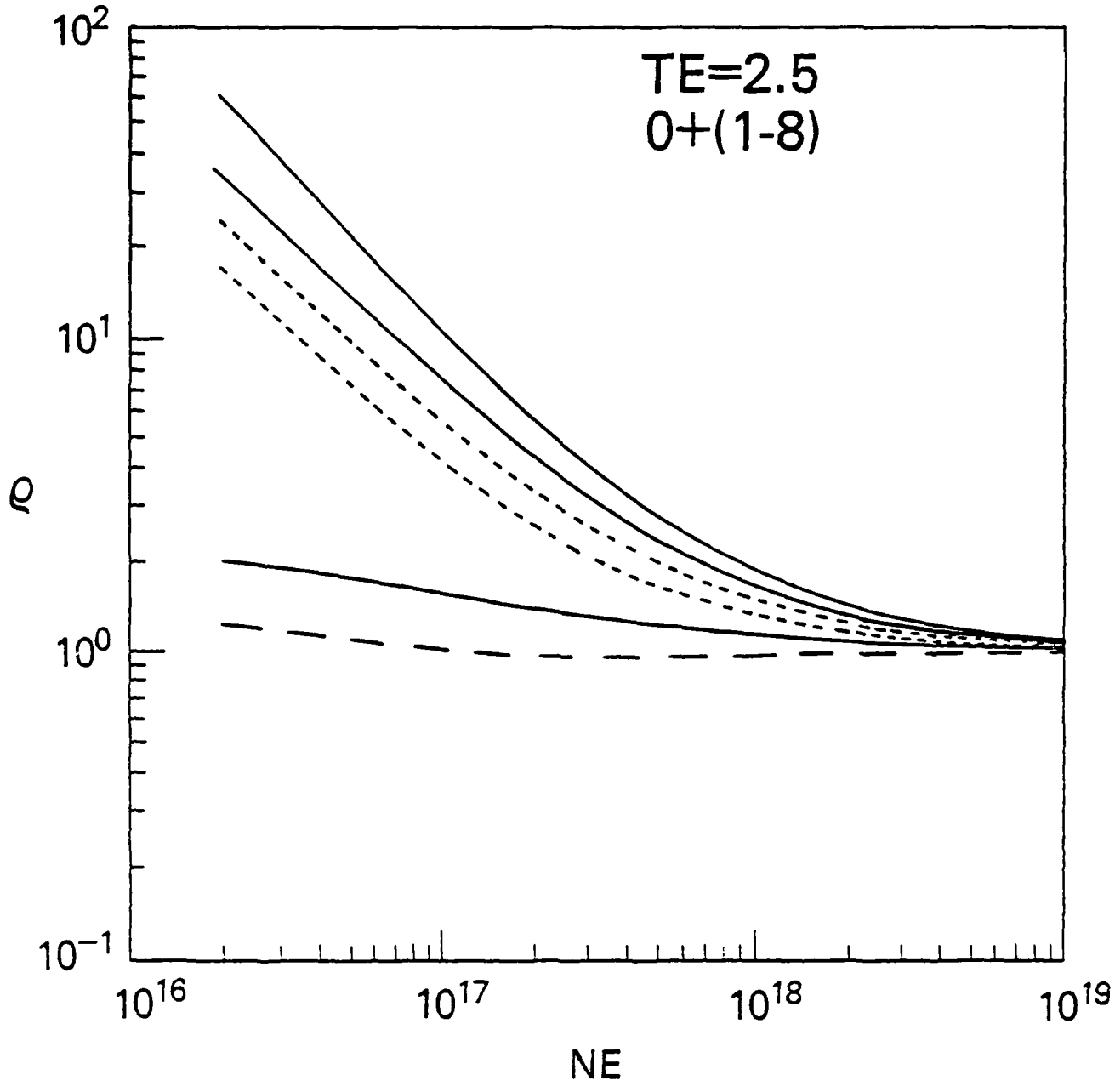

Fig. 15. Saha decrements, Te=2.5 eV; as in Fig. 7.

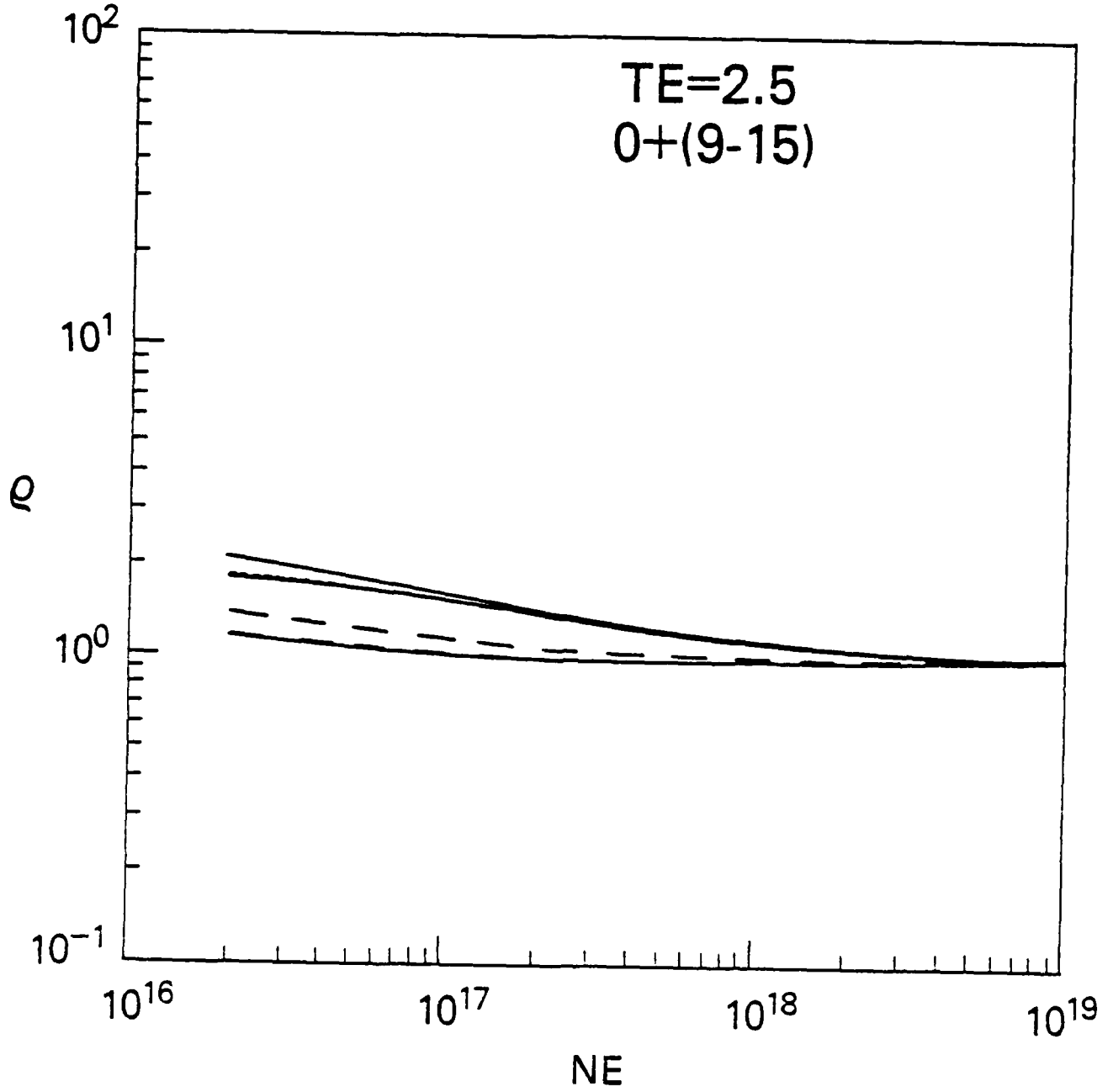

Fig. 16. Saha decrements, Te=2.5 eV. The initial order from top to bottom is $\rho^+(9)$, $\rho^+(13,15)$, $\rho^+(11)$ and $\rho^+(10,12,14)$.

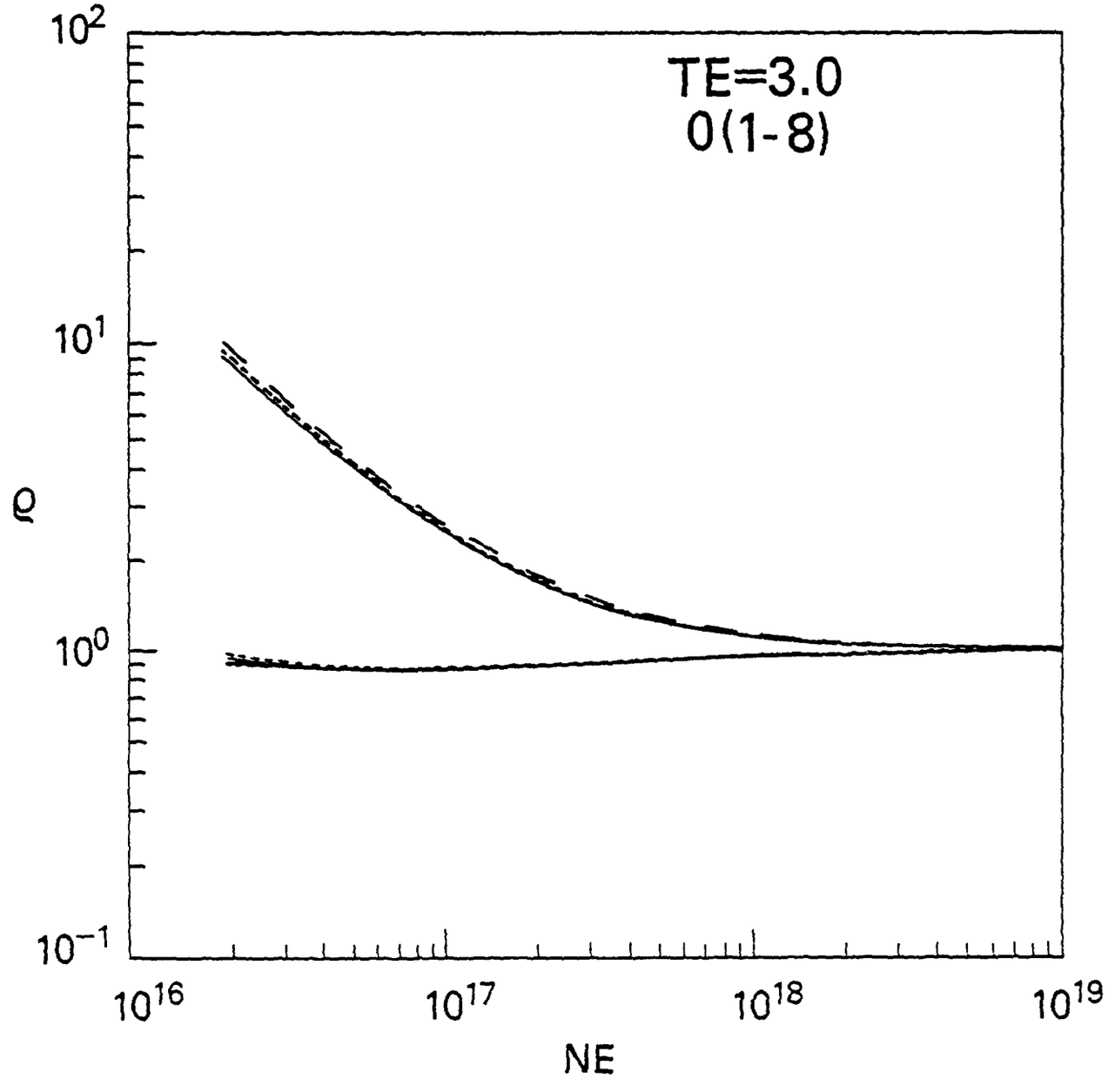

Fig. 17. Saha decrements, Te=3.0 eV; as in Fig. 9.

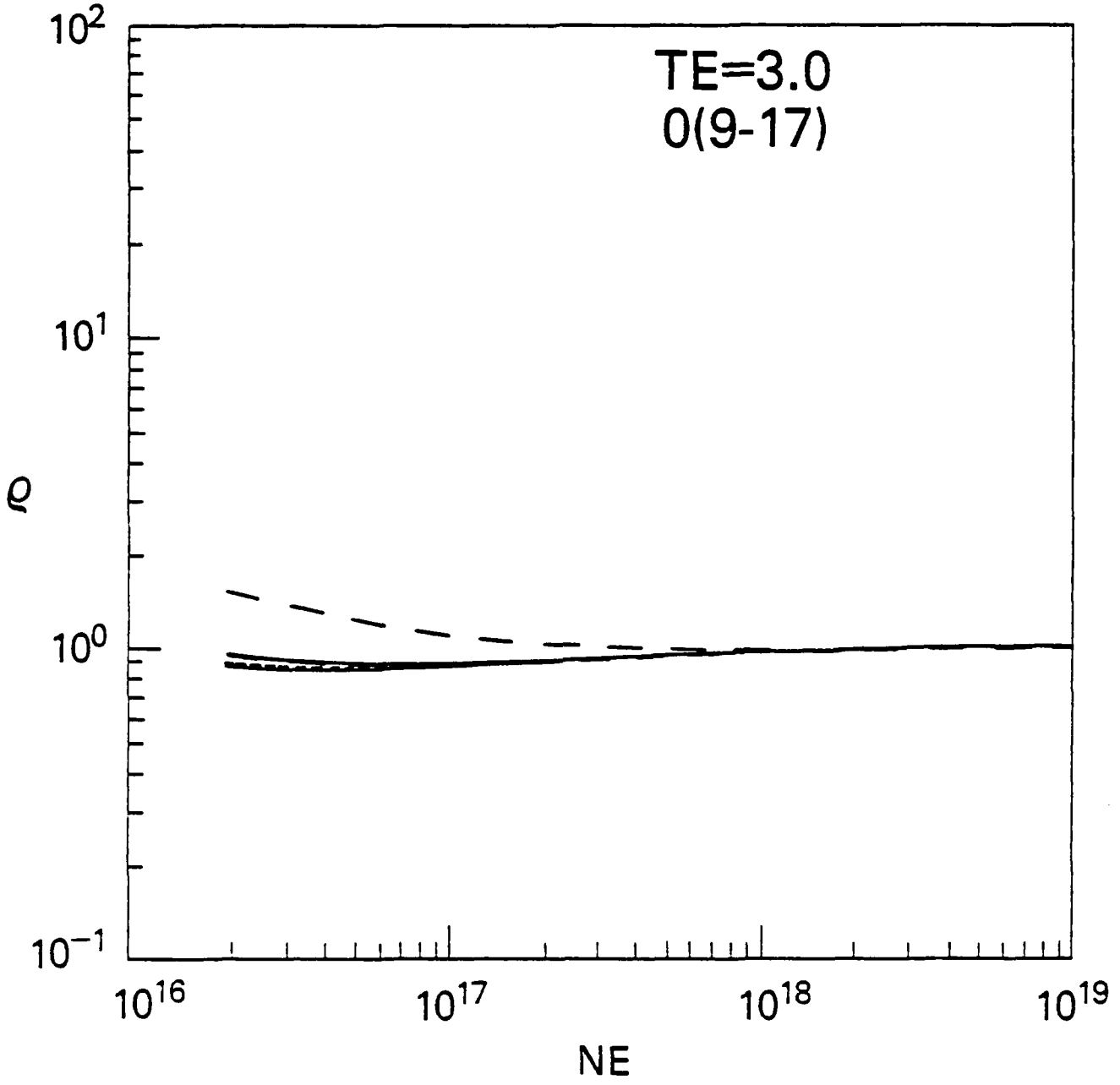

Fig. 18. Saha decrements, Te=3.0 eV; as in Fig. 14.

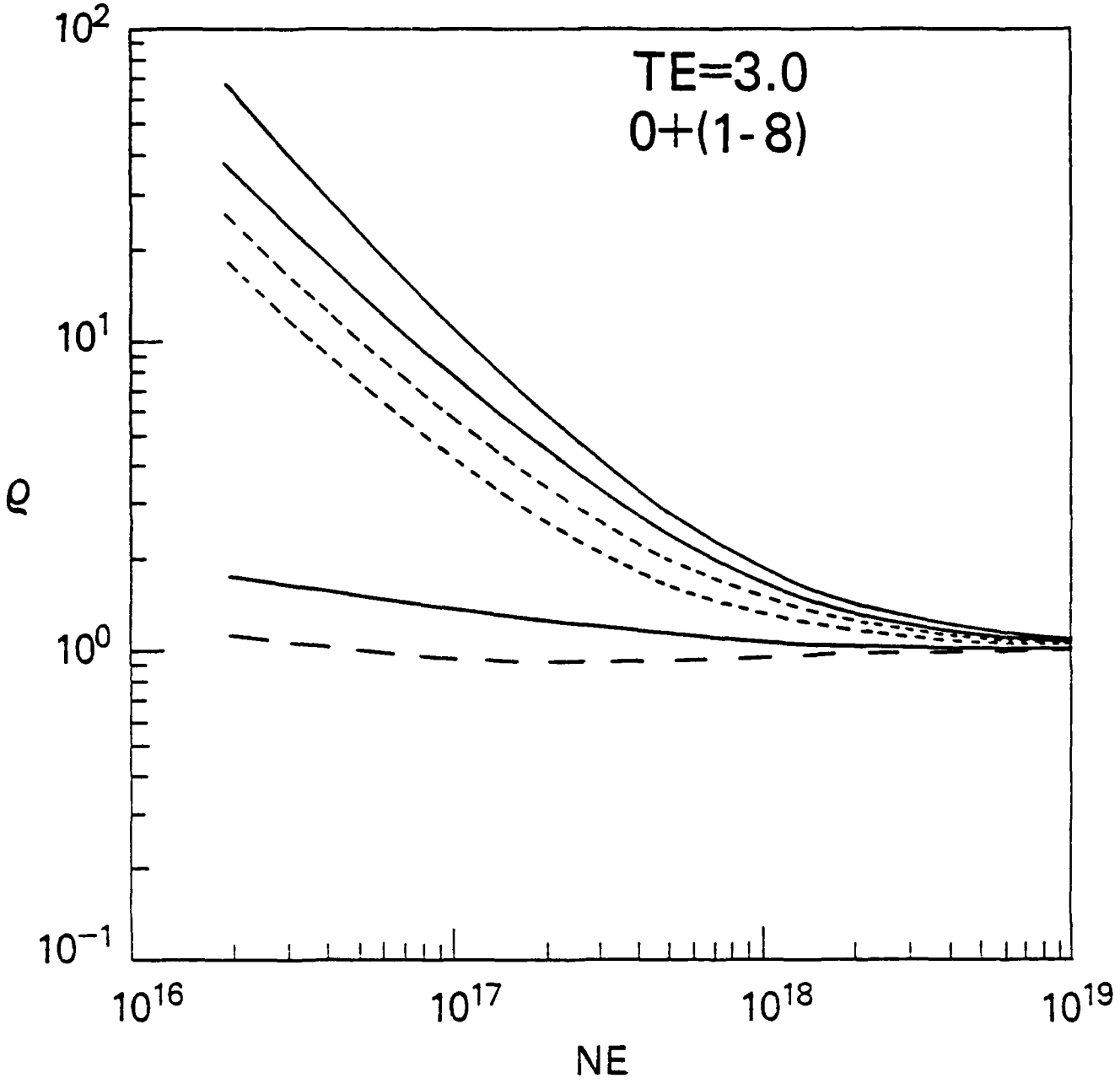

Fig. 19. Saha decrements, Te=3.0 eV; as in Fig. 7.

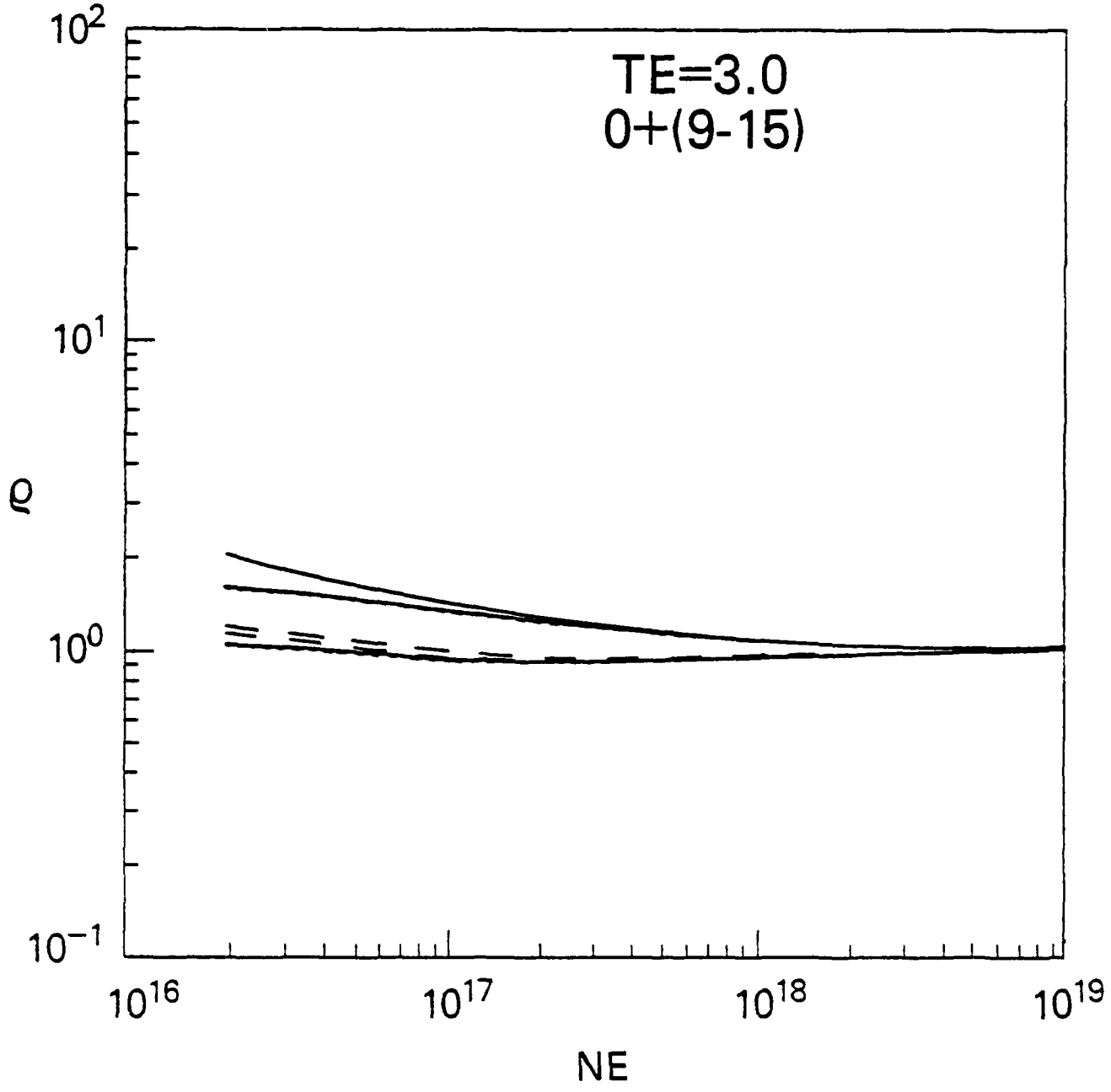

Fig. 20. Saha decrements, Te=3.0 eV. The initial order from top to bottom is $\rho^+(9)$, $\rho^+(13,15)$, $\rho^+(11)$, $\rho^+(14)$, and $\rho^+(10,12)$.

REFERENCES

1. R.D. Taylor and A.W. Ali, "Recombination and Ionization in a Nitrogen Plasma", NRL Memorandum Report 5594, Washington, D.C. (1985). ADA155426

2. Ronald D. Taylor and A.W. Ali, J. Quant. Spectrosc. Radiat. Transfer 34, xxxx (1985).

3. D.R. Bates, A.E. Kingston, and R.W.P. McWhirter, Proc. Roy. Soc. A267, 297 (1962); ibid. A270, 155 (1962).

4. D.R. Bates and A.E. Kingston, Planet. Space Sci. 11, 1 (1963).

5. D.R. Bates and A. Dalgarno, in Atomic and Molecular Processes, D.R. Bates, ed. Academic Press, New York (1962).

6. D.R. Bates and A.E. Kingston, Proc. Roy. Soc. A279, 10 (1964); ibid. 32 (1964).

7. W.L. Wiese, M.W. Smith, and B.M. Glennon, "Atomic Transition Probabilities", NBS Publication #NSRDS-NBS4, Washington, D.C. (1966).

8. A.W. Ali, R.H. Kummler, F.R. Gilmore, and J. William McGowan, Defense Nuclear Agency Reaction Rate Handbook (Edited by Bortner and Bauerer), DNA1948H, chapt. 20, DASIAC, DOD Nuclear Information and Analysis Center, Kaman Tempo, Santa Barbara, California, 2nd edition (1972) and revision 9 (1983).

9. H. Griem, Plasma Spectroscopy, McGraw-Hill Book Co., New York(1964).

10. L.J. Kieffer and G.H. Dunn, Rev. Mod. Phys. 38, 1 (1966).